Research Highlights 2003

In 2003 the style of the School's Annual Report has been changed substantially in response to changes in our publicity strategy and to better serve the University's central marketing objectives. The most significant change is the introduction of a Research Highlights section in lieu of lengthy Departmental reports. The rationale behind this is:

- The highlights serve as both promotional flyers and the basis for media releases.
- The Research Highlight posters and flyers do not necessarily become obsolete after one year as the previous style of report did.
- The flyers enable us to make tailored packages for visitors including stories about research in topics that may interest them, gathered from several years not simply the preceding year.
- Because new highlights are introduced to the report each year, the annual repetition from previous reports is avoided.
- Because researchers will only be asked to produce a highlight every few years the work load on academics is reduced, freeing them up to perform research.
- Likewise, because the Departmental Reports are now summaries, Heads of Department no longer have to write long reports each year. However, they do still have the opportunity to give an overview of their Department's activities and raise any issues they feel are pertinent.
- The shorter length and tailored versions of the new report have reduced printing costs by several thousand dollars.

The lengthy lists section detailing committees, service etc. are still being complied but will now be published in small numbers as an appendix, rather than in the main report. All this information will also be available on-line.

Dr Tim Wetherell

Quantum Supercomputer is a Step Closer

Matt Sellars, Jevon Longdell, Elliot Fraval, Annabel Alexander, Joanne Harison, David Pulford and Neil Manson

As the computer industry continues increasing the density of transistors on silicon chips a scale will be reach where quantum mechanical effects will introduce fundamental randomness into the chip's logic operations. This scale represents the ultimate limit for classical computing technology. These quantum effects whilst presenting a barrier also provide a way forward. Quantum computing attempts to control and exploit quantum effects not as means to cram more bits into silicon but to support a new kind of computation with qualitatively different algorithms based on quantum principles.

The potential power of quantum computing is a consequence of the large amount of parameters needed to fully define the state of a quantum system enabling a high density of information to be efficiently stored and manipulated. Consider a single bit, in a classical computer only one parameter is required to describes the state of the bit, which can be zero or one. However in a quantum computer the quantum bit or qubit can reside not just in the eigenstates of zero and one but also in coherent superpositions of these states. Two parameters are required to describe the wavefunction of a single qubit, an amplitude and a phase term. The number of parameters required rapidly increases with the number of qubits in the system. So for a two-qubit system eight parameters are required, where classically we would have expected two. By ten qubits the quantum/classical contrast is overwhelming, more than half a million parameters are required to describe what classically takes only ten.

The difficulty in realising a quantum computer is that the information contained in a quantum system is easily corrupted through uncontrolled interactions with the outside world. Somehow we must isolate our quantum system whilst still maintaining the ability to interact with it in a controlled manner. Due to the strong coupling of standard silicon transistors to their surroundings this requirement is likely to see the abandonment of silicon technology, for alternate technologies where the necessary high isolation can be obtained.

The Solid-State Spectroscopy Group in the Laser Physics Centre is developing quantum technologies based on the nuclear spins

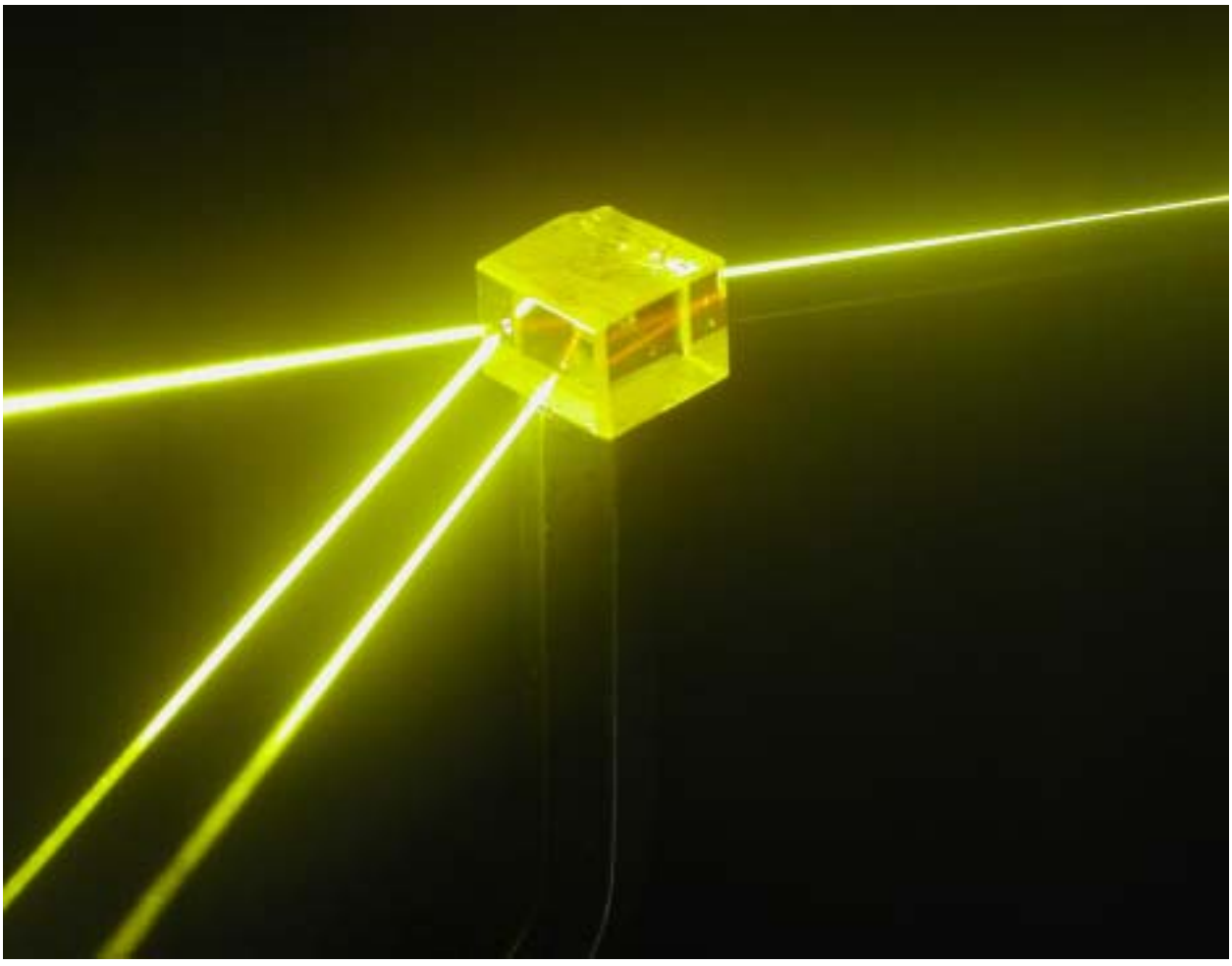

Eu^{3+} doped Y_2SiO_5 crystal refracts a laser beam

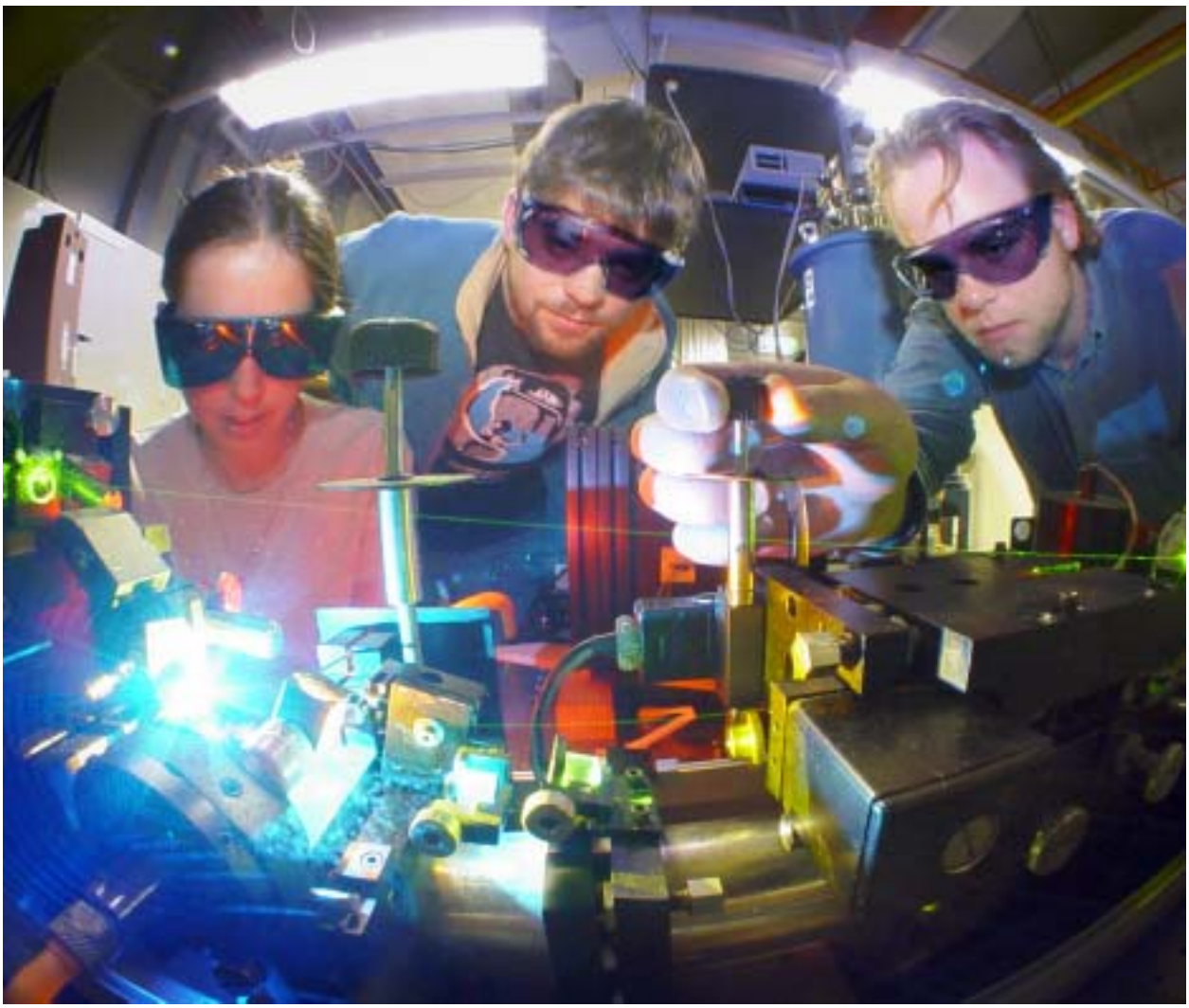

Joanne Harison, Jevon Longdell and Elliot Fraval make adjustments to one of the dye lasers in the spectroscopy/quantum computer labs

associated with optically active centers in solids. The approach allows the spins to be manipulated and measured using purely optical techniques, sidestepping the fabrication problems confronting other proposed solid-state architectures. In earlier work we demonstrated that the required high isolation of these nuclear spins from their environment could be achieved. A spin decoherence time of 82 ms was observed in Pr^{3+} doped Y_2SiO_5 with strong indications that decoherence times greater than a few seconds are attainable.

During 2003 the Group concentrated its efforts on demonstrating the control of the electronic states required to perform quantum operations. The procedure for manipulating the spins is to first transfer their quantum information to electronic states, manipulate these states using precise optical pulses and then return the information to the spin states. To demonstrate this control it is sufficient to demonstrate single and two qubit operations on the electronic states. In demonstrating these operations we performed the world's first two-qubit quantum logic operations based on solid-state impurity sites, along with a full quantum state tomography analysis of the single qubit gate operations. The two-qubit operation was only the second such demonstration in any solid state system.

The material chosen for the demonstration was Eu^{3+} doped Y_2SiO_5. It was selected because of the narrow homogeneous linewidth of the $^7F_0 \Leftrightarrow {}^5D_0$ transition associated with the Eu^{3+} ions at 579 nm, which can be as narrow as 100 Hz. The long coherence time associated with this narrow line width simplifies the implementation of the optical pulse sequences as it allows the use of microsecond time scale pulses to control the gate operations. These pulses can be generated by simple modulation of the output of a continuous wave laser.

A non-resonant electric dipole-dipole interaction between the ions was used to effect the two qubit operation. The Eu3+ dopant ion possesses a permanent electric dipole moment that depends on the electronic state of the ion and hence, exciting one ion induces a linear Stark shift in the optical frequencies of surrounding ions. The challenge in implementing quantum logic in Eu^{3+} doped Y_2SiO_5 is the need to select an ensemble of ion pairs with a relatively well defined interaction strength. This was accomplished by developing advanced optical pumping techniques. With this ensemble we demonstrated a phase shift in one qubit conditional on the state of the other (see figure 1).

Work is on the way to increase the fidelity of the gate operations and to scale the device up to more qubits.

Recording and Reading Three-Dimensional Optical Memory in a Transparent Solid

E. G. Gamaly, S. Juodkazis, A. V. Rode, B. Luther-Davies, H. Misawa

Recent improvements in the storage capacity of optical memories based on conventional CD-type surfaces are very impressive. For example, the new blue laser digital versatile disk, DVD, has a capacity of 27 Gbytes compared with current DVD capacity of 4.7 Gbytes. However, three-dimensional optical storage systems, where data is written throughout the volume of a recording medium rather than just on a surface, promise to far outstrip even this latest DVD technology by increasing storage capacity by more than 100 times.

In collaboration with our Japanese colleagues, Professors Hiroki Misawa and Dr Saulius Juodkazis from the Tokushima University, we have been working on a 3-D optical memory based on creating very small three-dimensional "data bits" with controlled size within a transparent solid. In our process a single short pulse of light from a laser tightly focused inside the solid modifies the material in a region only a few hundred nanometers in extent. Afterwards the presence of this "bit" of information can be detected (read) with another laser beam. Since these data bits are very small, they can be densely packed creating a storage density around 10Tb/cm^3 – a value comparable to holographic storage systems.

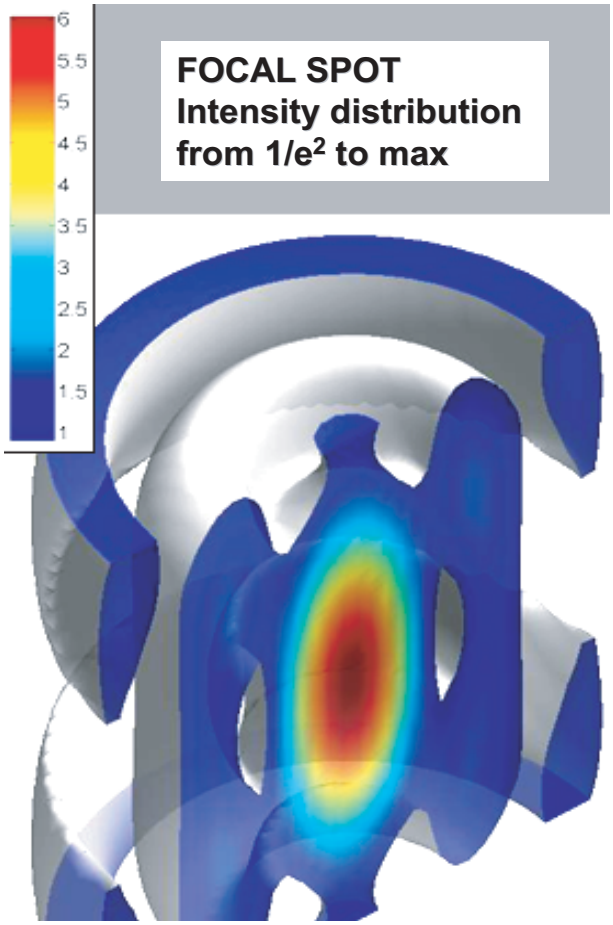

Intensity distribution of the focused laser spot

It is very difficult to write sufficiently small 3-D data bits using this technique but we were able to solve this problem because of our in depth understanding of the interaction of ultra-short laser pulses with materials. In particular we recognised that ionising the material in the focal spot to create plasma would restrict the volume in which the laser energy was deposited, and thereby the volume occupied by the data bit. We were, thus, able to define the optimum conditions for creating very small "bits" and demonstrate both writing and reading of data experimentally as part of a joint Japanese-Australian research program.

Interestingly the physics involved in "writing" a data bit closely mirrors what occurs during an underground nuclear explosion but on a scale some 25 orders of magnitude smaller in energy! When a short pulse of laser light is focussed tightly inside a solid to an intensity exceeding the optical breakdown threshold (≈6 10^{12} W/cm^2 for fused silica), high-density plasma forms almost instantly in the focal region. The original transparent glass is thus transformed into strongly absorbing plasma that concentrates the absorbed energy into a very small volume. The energy density now becomes so high that the pressure rises above the strength of the material and the local temperature also rises to around 20,000 K - well above that needed to break the atomic bonds. Thus the hot plasma at solid-state density starts to expand sending heat and shock waves into the surrounding material. Eventually a void is formed in the place where the laser beam was focussed and this becomes frozen into the material creating the data bit.

We applied a simple model based on strong explosion phenomenon within a solid to predict the size of the hollow void and obtained results in close agreement with experiments. Basically after the end of the laser pulse, the laser-heated dense gas expands adiabatically until its internal pressure drops to that in the surrounding cold material. By this time the gas density has dropped well below solid-state density and after cooling a void with predictable size remains surrounded by a region of compressed glass.

The presence of the structures could be "read" by collecting white light continuum generated from the laser-affected sites excited by femtosecond laser pulses at much lower laser intensity (10^{10} W/cm^2 – 10^{11} W/cm^2). The lateral and axial sizes of the void produced in silica glass at an intensity about three times higher than the breakdown threshold using 150 fs pulses at 800 nm were 259 nm and ~300 nm respectively – much smaller than the laser wavelength. Closer to the breakdown threshold the average size of the memory "bit" was 200 nm and the distance between adjacent bits could be reduced to 0.2 μm. A practical storage density for this memory was found to be around 10 Tb/cm^3.

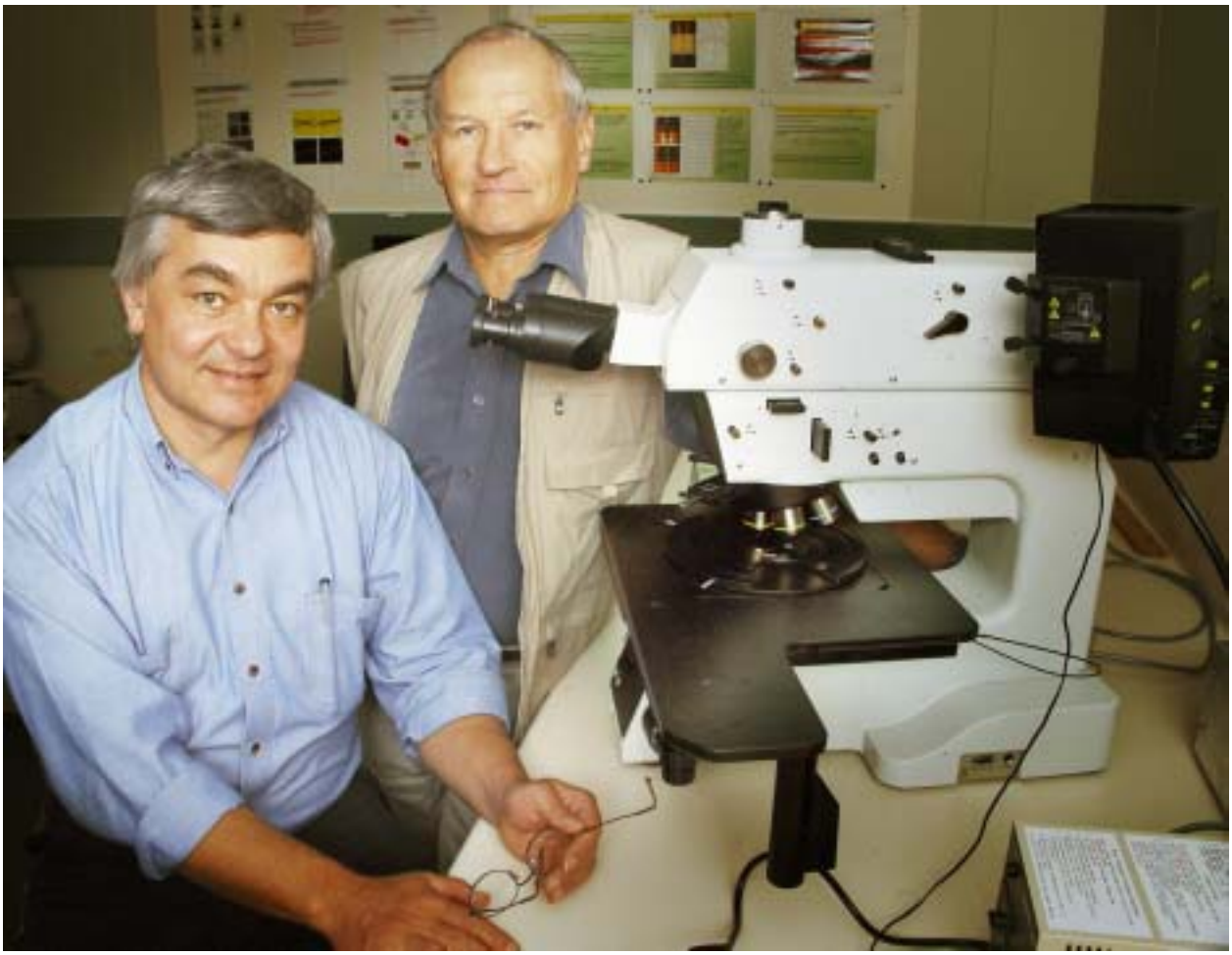

Dr Eugine Gamaly and Dr Andrei Rode (seated) with the confocal microscope used to characterise the laser induced cavities

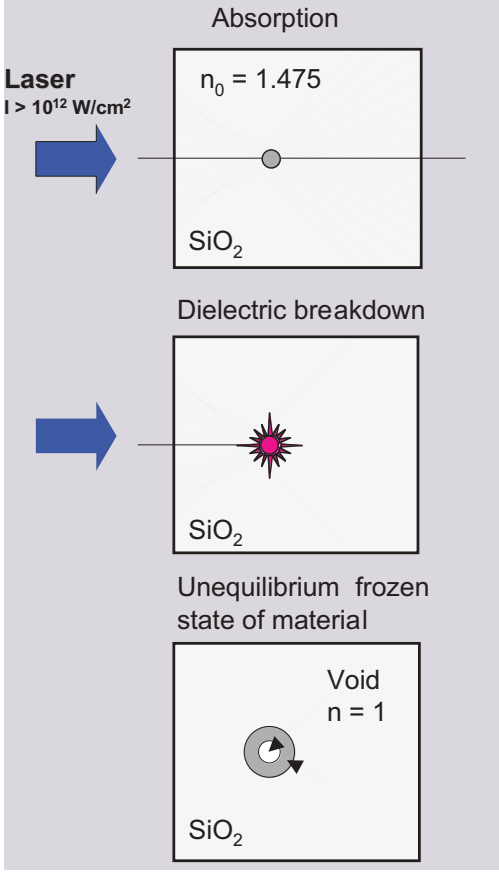

Images of 'bit' patterns recorded in the volume of fused silica glass by powerful 150 fs pulses and readout by white light continuum emission from the bits. The distances between the adjacent bits were 0.2 μm, 0.3 μm, and 0.4 μm. (Image courtesy S. Juodkazis).

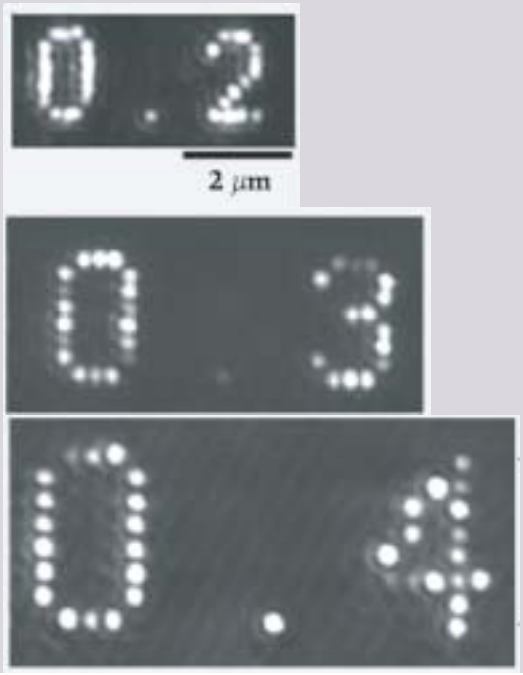

Electric Double Layer is Secret Behind Revolutionary Space Thruster

Christine Charles and Rod Boswell

Researchers at the Plasma Research Laboratory have discovered a supersonic ion beam coming from an expanding plasma. This ion beam is accelerated by a current-free electric double layer. Double layers are of great interest in astrophysics (aurora, solar corona, extragalactic jets...) and rocket science (electric propulsion for low orbit satellites and for interplanetary spacecraft).

One of the most beautiful mysteries in the heavens is the aurora which is seen during winter months at latitudes about 20 degrees away from the poles. These "lights in the sky" are caused by the impact of electrons with energies of a few kV on the upper atmosphere which excite various lines of oxygen and nitrogen resulting in the splendid colours and draperies. These displays have been observed and recorded for over two millennia but it was only in the last half of the 20th century that some light was shone on the basic plasma physics underlying the acceleration of the electrons to these high energies. The tools used to obtain the results were polar orbiting (or highly eccentric) satellites which passed through the active auroral regions in only a few seconds. One needed luck to have the satellite there when there was an active aurora. Rocket flights have also provided immensely useful data but suffered the same problem of "when to launch".

Over the past 25 years, it has become accepted that the basic mechanism underlying most of the observable phenomena was the existence of a large electric double layer situated about one earth radius (about 6000 km) above the visible auroral regions. An electric double layer is a local region in a plasma

Above: Members of the plasma thruster team gathered round the prototype

Left: The aurora, seen here from the northern latitude of Fife, Scotland

which can sustain a potential difference, much like a cliff of potential (like a riverwaterfall) that can energise charged particles falling through it. These double layers are rather exotic objects and are similar to collisionless shocks; they can only be described by resorting to non-linear physics. It is now recognised that they may play a major role in dissipation processes of solar flares. For example, some models of the current interruption mechanism leading to the production of solar flares invoke the existence of multiple weak double layers. Double layers are also thought to play a role in extragalactic radio emissions. In this case, particle beam driven wave instabilities on either side of gigantic double layer structures produce anomalous resistivity, maintaining a density cavity within which the double layer resides, creating optimal conditions for polarised radio emissions.

Electric double layers in plasmas have been studied experimentally, theoretically and by computer simulation. The majority of experiments reporting laboratory double layers generally fall into two types, current driven or current free double layers: the first involves creating two separate plasmas at different potentials and allowing them to interact in a central chamber joining the two sources with stable double layers being formed by careful manipulation of the external experimental parameters. It can also involve a current flow in cylindrical 'Q' machines or in DC discharges with an abrupt change in diameter. The second type involves a weakly magnetised system expanding away from a small source with the presence of a current free field aligned double layer. A few scientists have described experiments carried out in a pulsed system where the high potential in the upstream of the double layer was provided by the anode of the plasma source. However, for pressures above 5 x 10^{-5} Torr, no double layers were observed and above 4 x 10^{-4} Torr, no energetic ions were observed. Recently, in a research experiment called CHI KUNG, we have shown that a current free double layer can be generated in a plasma expansion in a magnetic field for pressures less than about 1 mTorr (Figure 1). A supersonic ion beam has been measured downstream of this double layer both for argon, hydrogen and oxygen discharges and to date there is no satisfactory theoretical analysis of this current-free double layer (Figure 2). The fascinating part is that the double layer is not triggered by forcing two plasmas (independantly generated by grids with separate potentials, much like a man-made dam) to interact, but self generates under certain parameters, much like the riverbed suddenly falling away to create a waterfall.

Apart from being an interesting phenomenon for space plasma physics, the ions accelerated by the double layer can be used for thrust in a space craft. Recently, there has been a renewed interest in plasma based thrusters for space applications and especially in non-gridded systems such as the Stationary Plasma Thruster or Hall effect thruster. This system uses a j x B type of plasma acceleration and was originally developed by the Russians: it is now being flown on spacecraft. Although no extraction grids are used, an electron source is still needed to properly neutralise the escaping ion beam.

A newly proposed system, magnetoplasma thrusters, uses plasma creation followed by perpendicular ion heating and adiabatic expansion to produce thrust (VASIMR at NASA). The ions need to be heated to some hundreds of eV perpendicular to the magnetic field and this is quite a challenge. The expansion of the plasma also provides up to 100 eV of energy from the electric field generated by the density gradient.

Our system presents a completely new phenomenon of a double layer in an expanding current free plasma to be used as the basis of a different genre of space plasma thrusters, the Helicon Double Layer Thruster (HDLT). We are currently building a prototype which will be tested at ESA (European Space Agency) in Europe. It is simple, has no moving parts, no electrodes and no need for a neutraliser. Both the research (CHI KUNG reactor) and development (HDLT prototype) efforts are being carried out in parallel by a team of scientists and Ph D students in collaboration with astrophysicists, rocket physicists, and plasma physicists around the world (USA, France, Norway, Sweden, Germany...).

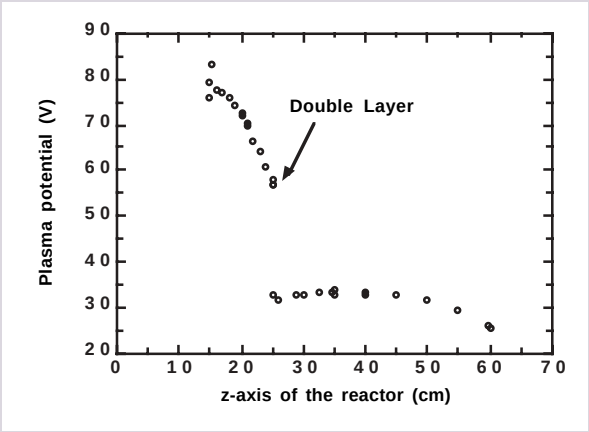

Figure.1: Potential drop at ~25 cm showing the double layer

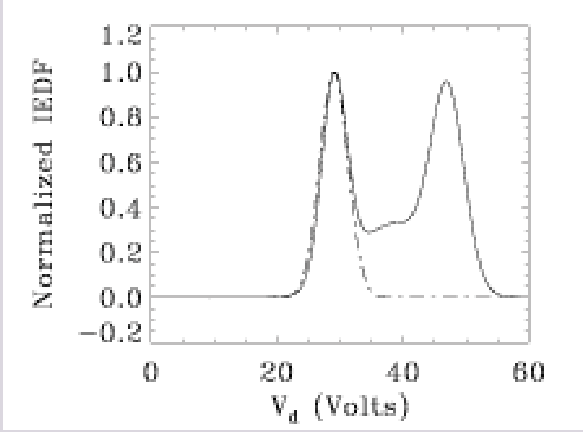

Figure. 2: Radial (facing the walls/dotted line) and axial (facing the double layer/solid line) Ion Energy Distribution Functions downstream of the double layer, showing the supersonic ion beam at high energy.

Taking the Strain out of Quantum Lasers

Hoe Tan, Penny Lever, Kallista Stewart, Fu Lan, Qiang Gao, Sudha Mokkapati, Satya Barik, Michael Fraser, Greg Jolley, Manuela Buda, Jenny Wong-Leung and Chennupati Jagadish

Semiconductor quantum dots (QDs), such as InGaAs on GaAs substrates, are typically formed by the Stranski-Krastanov process where the lattice mismatch between the material being deposited on and the substrate cause the formation of islands of nm size to relieve the excess energy. Arguably, the best III-V quantum dots are grown by Molecular Beam Epitaxy (MBE), where this high vacuum deposition technique allows a myriad of electron beam techniques to observe in-situ the formation of the dots. Hence, the control of the QD formation is very precise. In metal organic chemical vapour deposition (MOCVD) technique, the in-situ monitoring techniques is limited. Furthermore, deposition in MOCVD is typically done at higher temperature (50-100°C) than MBE due to precursors used in MOCVD that require higher temperature to pyrolise. The higher growth temperature is not favourable in the QD formation due to enhanced mobility of the In adatoms. Nevertheless, reasonable quality InGaAs and InAs QD structures have been grown by MOCVD as reported in several international laboratories.

In most optoelectronic devices with QDs, it is generally required to grow a number of QD layers as a stack on top of each other to increase the optical gain (such as for lasers) or the absorption volume (such as in detectors). However, since these QDs are highly strained material, the gradual accumulation of strain by stacking these layers could lead to relaxation which result in QDs with dislocations/defects and degrade device performance. Hence we need to investigate ways to suppress the strain build up while increasing the number of stacked layers. Furthermore, typically in optoelectronic devices that utilise QDs, optical cladding layers, such as AlGaAs, need to be grown after the formation of these QDs. These cladding layers needs to be grown at higher temperatures to get good quality material but the temperature has profound effect on the atomic diffusion and the dissolution of the QDs. As such a compromise in the growth temperature of the cladding layers need to be found.

We have demonstrated, by MOCVD process, the number of InGaAs QD layers could be increased by (a) improving the quality of the barrier layer in between the QD layers and (b) by introducing strain compensation layers in the vicinity of the QD layers. In the former technique, growth interruption, i.e. a temporary stoppage of deposition, was introduced to further let the shape of the InGaAs QDs evolve and stabilise followed by the deposition of GaAs barriers with a high V/III ratio to achieve smooth surface. In the latter technique, a very thin layer of pseudomorphically-strained GaP layer was grown very close to the QD layers. Since GaP has a smaller lattice constant than GaAs, an opposite strain effect will compensate the strain caused by the formation of the InGaAs QDs. Hence, the free energy of the system is reduced. Using both techniques, we managed to grow 15 layers of stacked QDs with good optical properties.

We have also successfully grown AlGaAs cladding layers at much lower (600-650°C) than normal growth temperature (700-750°C) without sacrificing too much on their quality. This was done with by introducing carbon tetrachloride (CCl_4) during the growth of AlGaAs where we postulate that the CCl_4 removes the impurities/defects created during low temperature growth. Furthermore, the carbon atoms in CCl_4 also act as p-type dopants in AlGaAs which are required to form electrical path/contact.

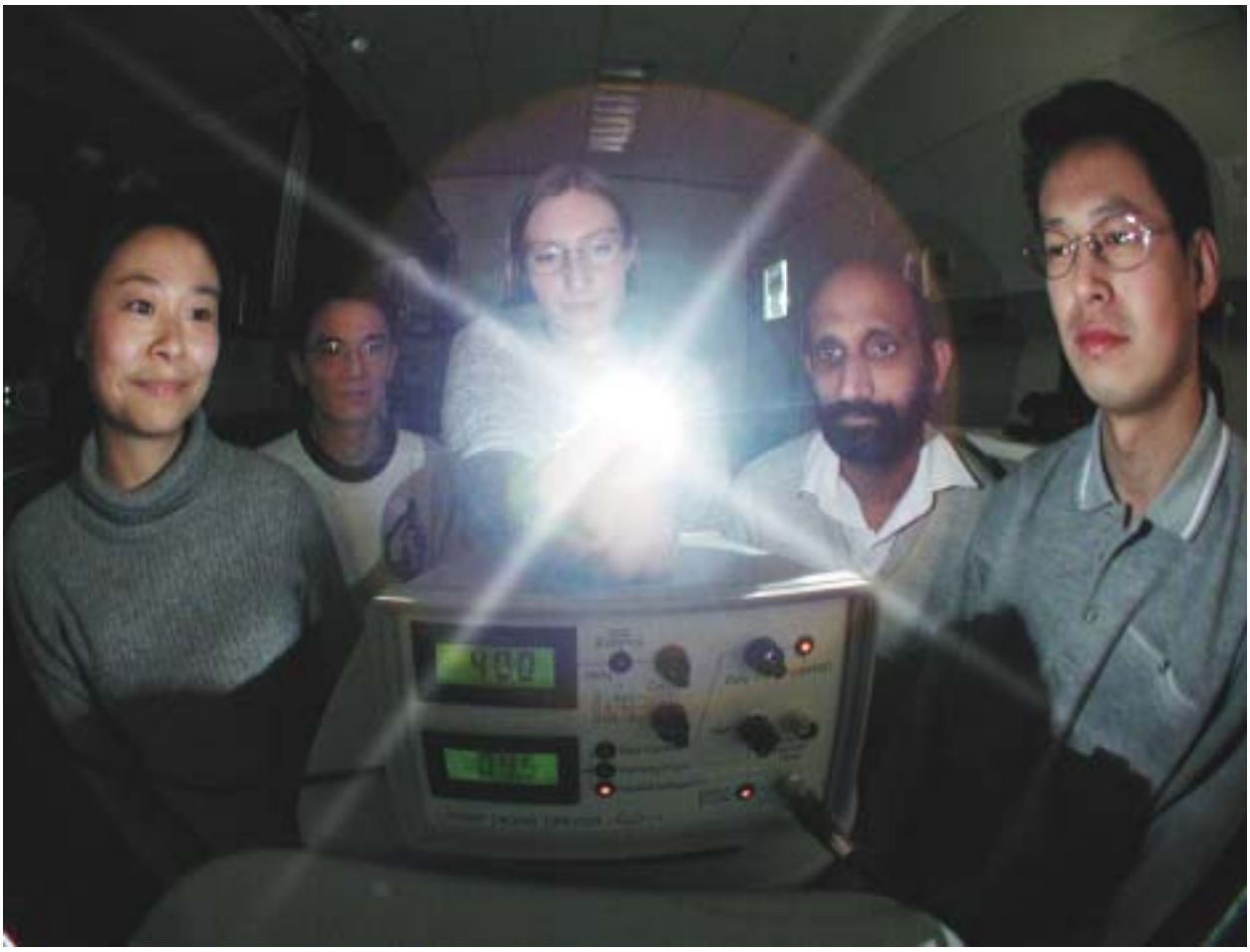

By using the combination of these techniques, we have demonstrated the operation of InGaAs QD lasers. It is worth mentioning here that although QD research has been on-going for the past decade or so, only a handful of groups in the world reported the successful operation of QD lasers grown by MOCVD. The optimised (with smoothing and GaP) devices showed a marked improvement in the efficiencies over reference devices. We also observed lasing in both the ground state and excited states for the QD lasers for devices with different cavity lengths. These devices lased at around 1080-1150 nm. In addition to broader emission peaks from QD lasers compared to QW devices (due to inhomogeneous spectral broadening caused by the QD size variation), modulation in the lasing spectra was observed. This has been attributed to the leaky modes in the substrate. Wavelength shifted devices have also been demonstrated just by simple thermal annealing due to the lower temperature stability of the QDs. In addition to InGaAs QDs, we have also managed to grow InAs and InGaAsN QDs with emission at 1300 nm. Further experiments are now underway to grow these QDs in laser structures to obtain lasing at ~1310 nm, which is the wavelength of interest for optical communication applications.

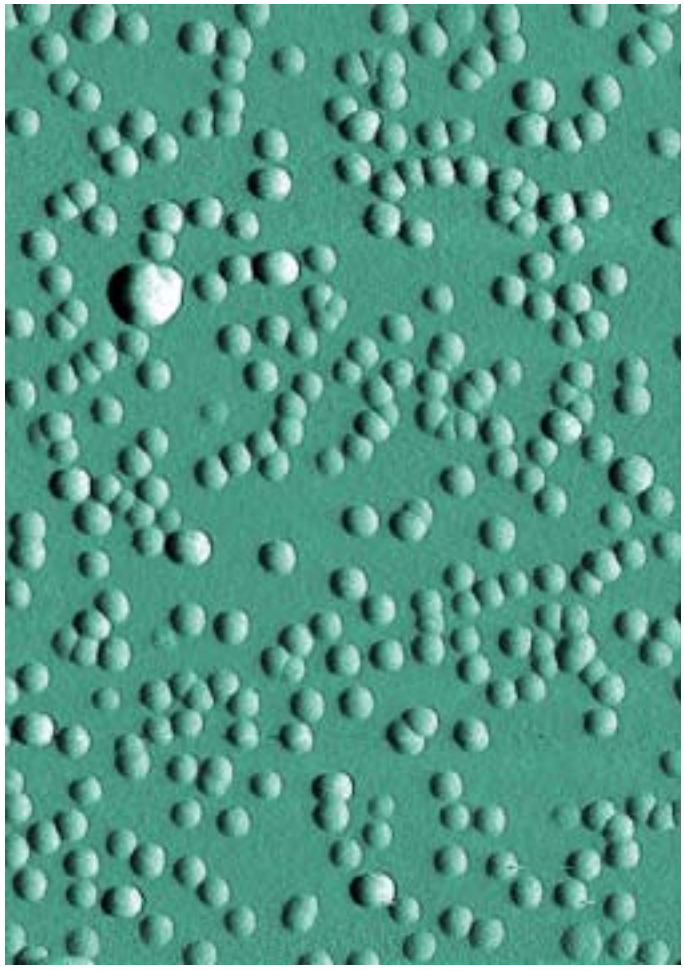

Above: Members of the quantum laser team
Left: the MOCVD reactor is maintained under slight positive pressure to eliminate atmospheric dust
Right: Microscopic quantum dots on the surface of crystal semiconductor

Theoretical Studies of Ionic Channels

Shin-Ho Chung, Megan O'Mara and Taira Vora

The long-term goal of the Biophysics Group in the Department of Theoretical Physics is to provide a comprehensive physical description of biological ion channels. Such a theoretical model, once successfully formulated, will link the structure and function of ion channels through the details of the inter-molecular potential operating between ions, water molecules and atoms that form the channel. Because all electrical activities in the nervous system, including communication between cells and the influence of hormones and drugs on cell function, are regulated by the opening and closing of ion channels, understanding their mechanisms at a molecular level is a fundamental problem in biology. Moreover, elucidation of how single ion channels work will ultimately help us find the causes of, and possibly cures for, a number of neurological, muscular and renal disorders.

During the past several years, there have been enormous strides in our understanding of the structure-function relationships in biological ion channels. This sudden advance has been brought about by the combined efforts of experimental and computational biophysicists, who together are beginning to unravel the working principles of these exquisitely designed biological macromolecules which regulate the ionic gradients across the living membrane. In recent breakthroughs made by Rod MacKinnon and his colleagues, the molecular structures of several different types of ion channels have been determined from crystallographic analyses. In parallel to these landmark experimental findings, there have been important advances in computational biophysics. As new analytical methods have been developed and the available computational power has increased, theoretical models of ion permeation have become more sophisticated.

In building a theoretical model of biological ion channels, we utilise a combination of macroscopic calculations, semi-microscopic stochastic dynamics and fully microscopic molecular dynamics simulations. We first construct a simulation assembly, composed of all the atoms forming an ion channel, a large reservoir which is connected to each end of the channel to mimic the extracellular or intracellular space, and a fixed number of anions and cations in the reservoirs. The electrostatic forces experienced by the ions in the assembly are obtained by solving Poisson's equation satisfying the Dirichlet boundary condition. Then, we follow the trajectories of the ions by performing stochastic dynamics simulations. In these simulations, we solve the dynamical equation of motion in classical mechanics, known as the Langevin equation, for each ion at a fixed time to determine where it would have moved to after a short time interval. This calculation is performed many billions of times to deduce the

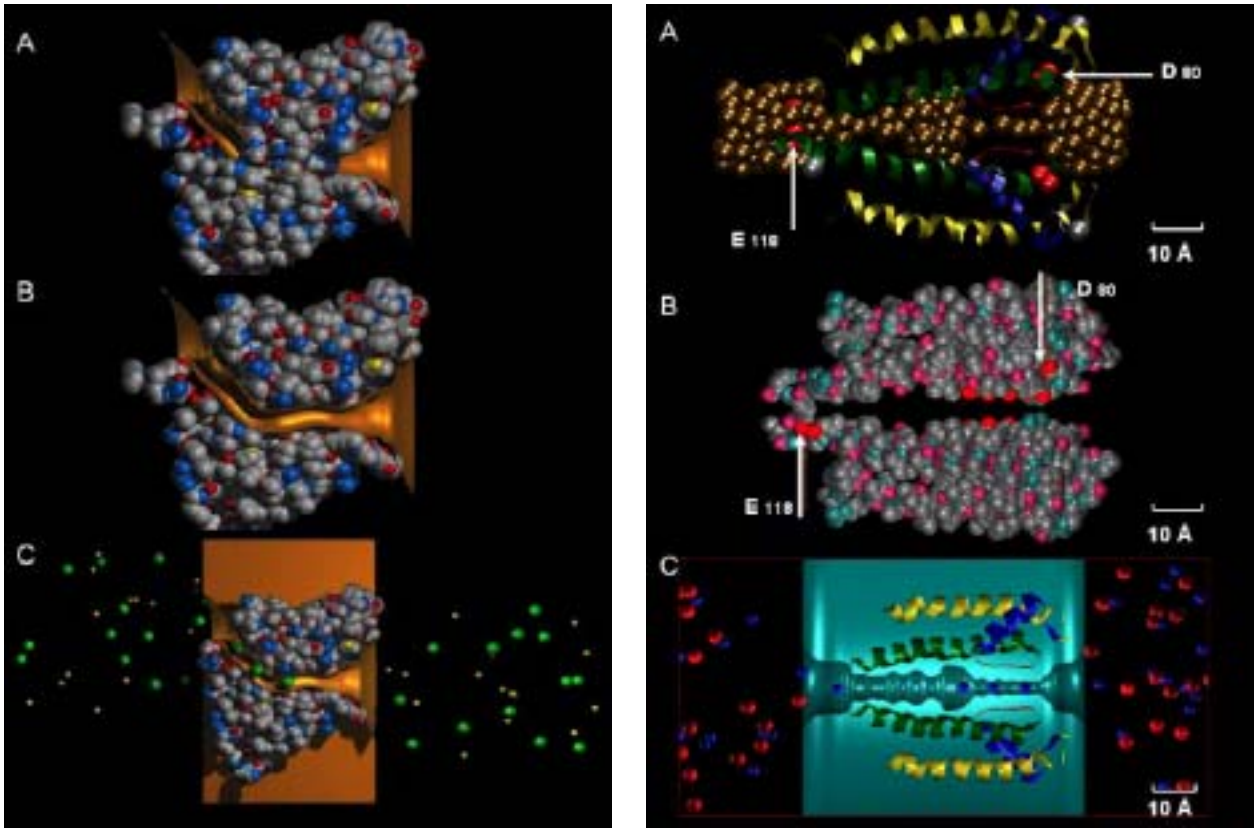

Theoretical models of ion channels. figure 1 (left) and figure 2 (right) see main text for detailed explanation

macroscopic properties of an ion channel. Some of the parameters that are needed to carry out stochastic dynamics simulations are calculated by employing classical molecular dynamics simulations.

Using the principles of classical electrodynamics and Newton's law, we have elucidated the dynamics of ion permeation across ClC-type chloride channels. The ClC family of chloride channels, present in the cell membranes of every living organism, performs diverse physiological roles, from the control of cellular excitability, acidification of intracellular vesicles, to the regulation of cell volume. Because the crystal structure of the bacterial ClC channel reported by MacKinnon and his colleagues is in a closed state (Figure 1a), we first re-model the protein to create an open-state configuration with molecular dynamics (Figure 1b). Then, retaining the same pore shape, the prokaryotic ClC channel is converted to several eukaryotic ClC channels by replacing all the nonconserved dipole-containing and charged amino acid residues. A model so created, with the front half of the atoms removed to reveal the pore (in gold) is shown in Figure c. For the system used for stochastic dynamics simulations (Figure 1c), the protein is incorporated in a low dielectric region representing the membrane (gold), and Cl^-(green) and Na^+ (yellow) ions are added to the reservoirs on each end. Employing open state eukaryotic channel models, current-voltage-concentration profiles consistent with experimental measurements are obtained. We locate the binding sites, as well as pinpointing the rate-limiting steps in conduction, and unravel the dynamics of ion permeation across the pore.

Following the same procedure, we have also successfully produced a model of the potassium channel, which is responsible for maintaining the membrane potential across the cell membrane. Two of the four subunits of the experimentally determined protein and the positions of water molecules inside of the pore are illustrated in Figure 2a. An outline of the water-protein boundary of the potassium channel, smoothed with a water molecule, is shown in Figure 2b. For stochastic dynamics simulations, a reservoir is attached at each end of the channel and a fixed number of K+ (blue) and Cl- (red) ions are placed in each reservoir (Figure 2c).

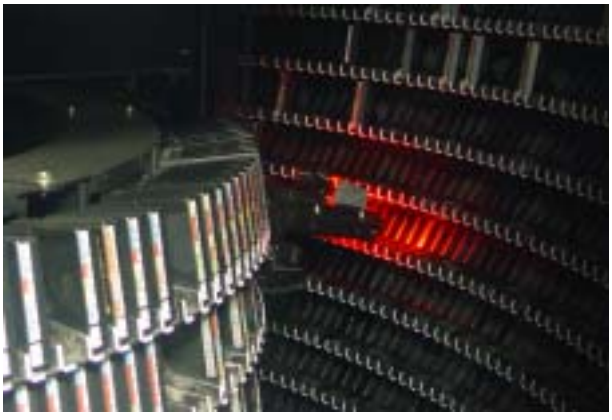

Above: Data storage tapes in the supercomputer facility
Top: Taira Vora and Megan O'Mara

The Last Ice Age in Australia: Exposure Dating Using the Heavy-ion Accelerator

Timothy Barrows , Keith Fifield, Accelerator Mass Spectrometry Group

The technique of "exposure dating" is arguably the most significant new dating tool introduced to the earth sciences in recent years. Dr Timothy Barrows of the Accelerator Mass Spectrometry group (led by Dr Keith Fifield) is using this technique to take a fresh look at the history of glaciation and climate change in Australia over the last million years.

Exposure dating is based on the principle that long-lived radioisotopes ("cosmogenic isotopes") accumulate naturally at the Earth's surface as a result of interactions between extremely high-energy cosmic rays from interstellar space and atomic nuclei in surface rocks. The two principal radioisotopes are beryllium-10 and chlorine-36, which have half-lives of 1.5 million years and 300,000 years respectively. They are produced by nuclear reactions between cosmic rays and oxygen and potassium or calcium nuclei in the rock. After a geological process freshly exposes a rock surface, these cosmogenic isotopes build up at a constant rate. Measurements of their present-day abundances, in conjunction with knowledge of the rate at which they are produced, allow an "exposure age" of the surface to be determined. This technique is powerful, because it allows the direct dating of features as diverse as glacier advance and retreat or volcanic eruptions.

Concentrations of cosmogenic isotopes in typical earth materials are incredibly low, being less than one in a million million (10^{-12}) relative to their stable counterparts. Hence, the ultra-sensitive technique of accelerator mass spectrometry (AMS) is required. The powerful and versatile 14 million volt 14UD tandem accelerator in the Department of Nuclear Physics has proved to be one of the best in the world for such measurements. This is an excellent example of the way in which instrumentation and expertise developed for basic research in one field can lead to new and interesting capabilities in a quite different area of research, and highlights the value of facilities like the 14UD accelerator where the range of research promotes such symbioses.

Exposure dating forms the basis of a rapidly expanding field and is leading to exciting discoveries. The biggest impact of exposure

A very large boulder on the inner terminal moraine at Blue Lake. This was plucked from the underlying bedrock or fell onto the glacier and was transported by the flowing ice to its present position. A sample for exposure dating was collected from the top surface. The rock is put through a sophisticated chemical procedure that reduces the ~1 kg of rock to 0.5 mg of beryllium oxide for the ion source of the accelerator. Our dating shows that this boulder was deposited here 20,600 years ago.

Blue Lake in the Snowy Mountains of Australia. The lake was excavated by a 150 m thick glacier that flowed to the right of the photo down towards the Snowy River.

dating is within the field of glacial geomorphology. Here it has revolutionised the way we study the history of glaciers and ice sheets. By directly dating glacial debris and eroded bedrock, the timing of the advance and retreat of the ice can be determined with unprecedented reliability. Glaciers are very sensitive indicators of climate, and hence this has a direct bearing on how well we know the behaviour of the climate in the past, and by implication, how well we will be able to predict it into the future. Previously, it was necessary to rely upon radiocarbon dating of organic material in glacier deposits. Often this material bore no direct relationship to the advance and retreat of the ice itself.

Exposure dating is being applied extensively by Dr Timothy Barrows of the AMS group to the study of relics of the last Ice Age, particularly in the Snowy Mountains and Tasmania. These studies have led to a complete revision of the glacial history of these regions, which were the only areas in Australia where glaciers existed. Hypothetical ideas about glacier extent and its timing that stood for nearly a century have been replaced with a robust chronology placing Australia into a global context. It transpires that there was not just one but at least four major advances of glacier ice during the last 70,000 years, and these have been named after the Kosciuszko Massif where he first recognised them. The best example of glacial activity is at Blue Lake, where there is a well-developed sequence of moraines, ridges of debris scoured by the glacier from its bed and deposited at its positions of maximum advance or along its flanks (see picture). Other locations studied include Cradle Mountain, Lake St Clair, and the Mt Field National Park, all in Tasmania, and tell a similar story to that in the Snowy Mountains.

In addition to glacial landforms, periglacial landforms are abundant in Australia (present even on Black Mountain in Canberra), a legacy of much colder temperatures during the Ice Age. These are landforms created by the action of frost, snow and ice under freeze-thaw conditions where glaciers are not present. They often take the form of block—'aprons' below a cliff face, or as block streams extending downhill away from the cliff. Because they are so indicative of temperature change, they are important features to date. Dr Barrows has pioneered a way to date these landforms using exposure dating. By studying typical deposits in southeastern Australia and Tasmania, he has determined that the youngest periglacial deposits formed during the height of the last Ice Age, 22,000 years ago.

Through Dr Barrows' research on dating of cold climate landforms we have learnt a great deal about when major temperature changes occurred in Australia. The coldest part of the last ice age was 20,000-22,000 years ago and only lasted a few thousand years. The ensuing global warming is the greatest in recent geological history. Using the altitude of the ice age landforms we have calculated that mean temperatures around Canberra are about 9°C warmer today. This research provides an important baseline from which to assess climate variability and raises intriguing questions about the adaptation of Aboriginal people to the conditions at the time.

Materials Science Questions Pedigree of Martian Bugs?

Stephen Hyde, Anna Carnerup, Andy Christy and Ankie Larsson

There is no doubt that materials made within living organisms remain far more advanced than the most lauded "advanced materials" humans can synthesize in the lab. It has been pointed out years ago, and remains true today, that a humble blade of grass far exceeds any synthetic material in its resistance to fracture and ability to withstand extreme stresses without failure.

Scientists at the ANU have been studying the fundamental processes behind biological structures in the hope of discovering their secrets and applying them to advanced synthetic materials. However this work has also had an interesting spin off.

ANU scientists have been able to make very complex structures in the lab that closely resemble what were assumed to be microfossils in natural rock.

The syntheses are very simple, requiring only a source of carbonate ions (e.g. atmospheric CO_2), strong alkaline aqueous solutions, silica and rare earth cations (Ba and Sr, Ca at high T) - all common ingredients in early planetary formation.

This discovery has profound implications for our understanding of early life on Earth. It also casts a different light on worm like structures in the Martian meteorite found in Antarctica. The ANU synthetic silicates bear an uncanny similarity to the Mars microbe!

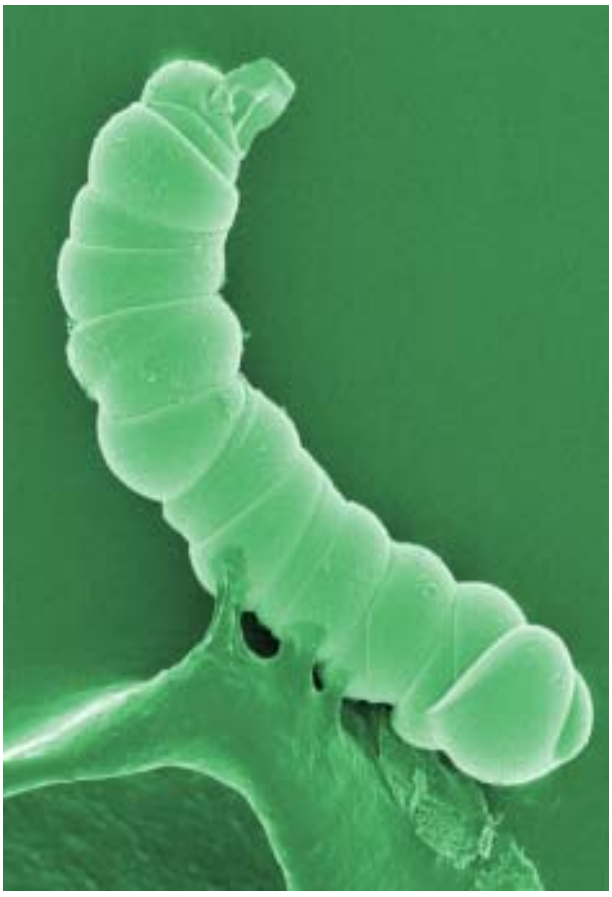

Above: Red planet or dead planet? Mars
Above right: one of the presumed Martian fossils
Right: Synthetic silicate grown under totally sterile conditions in ANU labs
Opposite right: Anna Carnerup and Stephen Hyde in the optical microscopy lab
Opposite below: some of the many exotic and beautiful silicates grown under different conditions

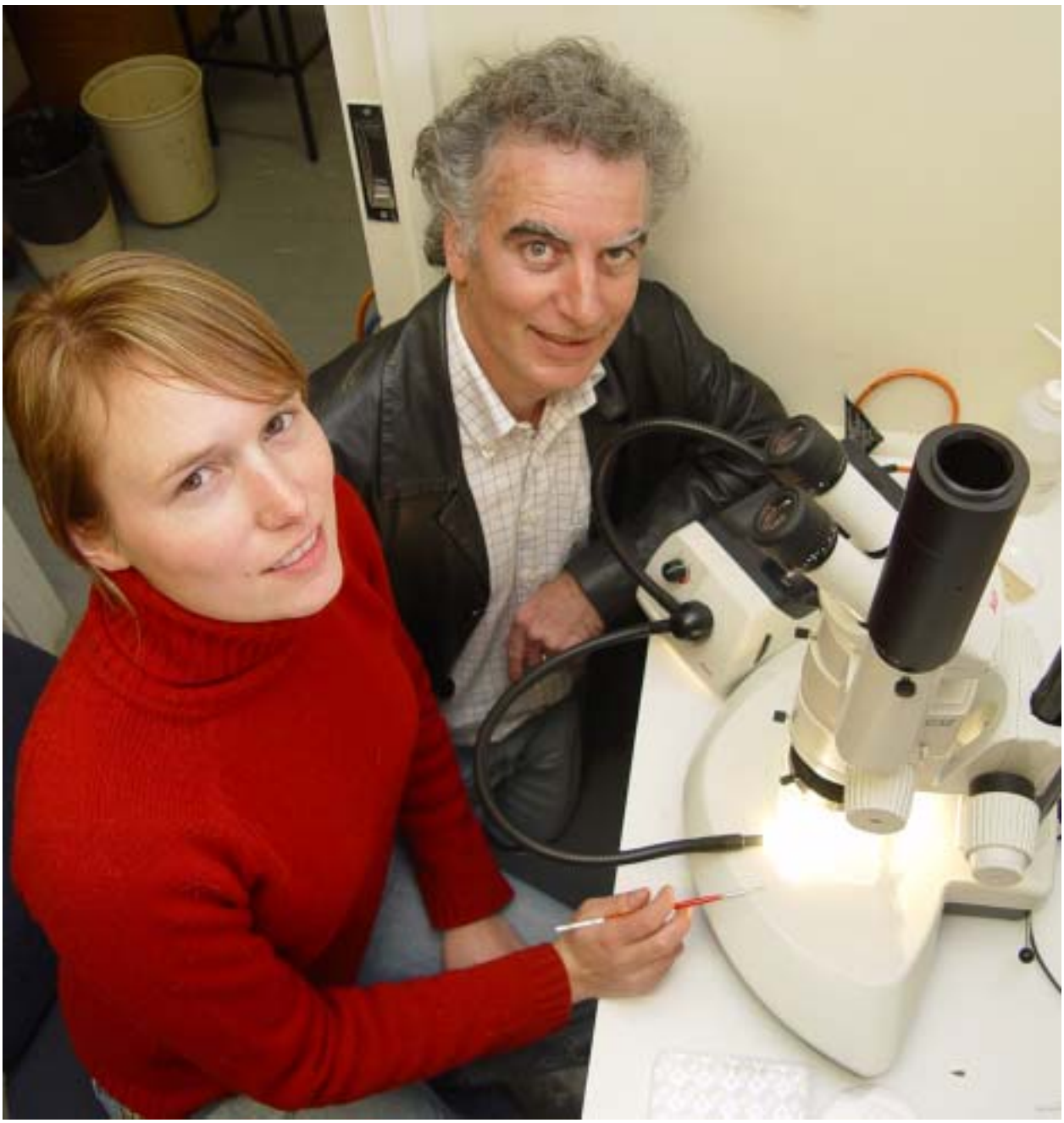

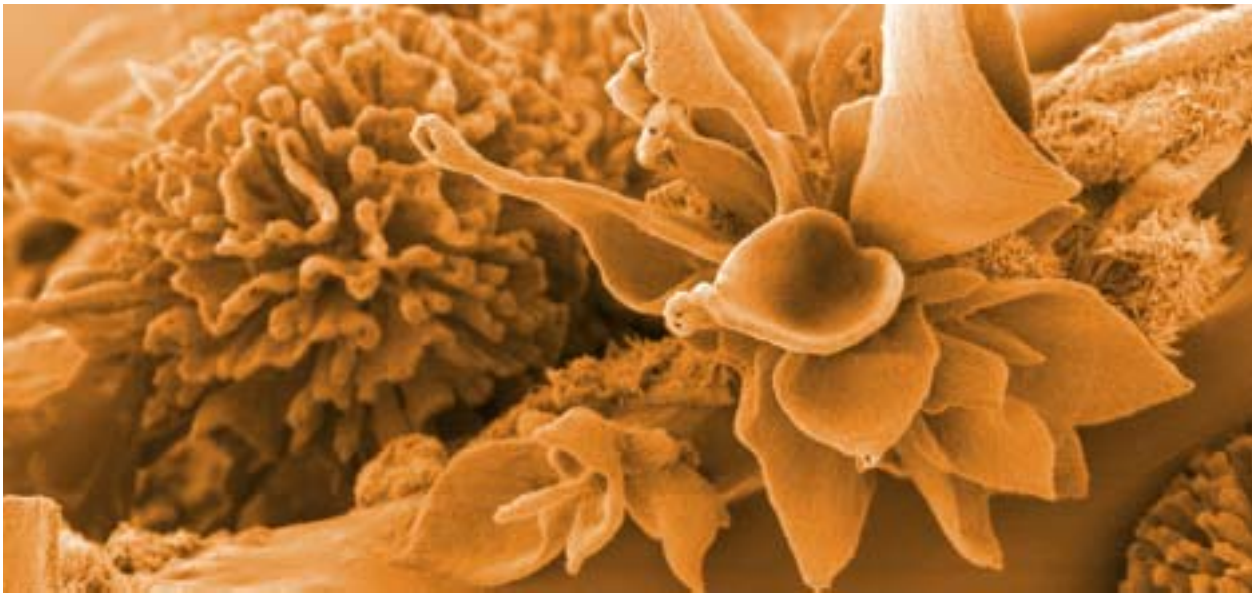

New Bend Loss Model Widens Optical Fibre Applications

Adrian Ankiewicz and John Love

During the last two decades of the twentieth century, single-mode optical fibres rapidly became the backbone of the world's vast telecommunications network both on land and under the oceans because of their ability to propagate large volumes of digitised data over vast distances with minimal light loss and signal distortion. The fibres are normally encased in optical cables to protect them from environmental hazards, but these cables, such as the one shown in the picture, are sufficiently flexible so that they can be bent into the small radii of some tens of centimetres that are encountered when they are laid in ducting under city streets and elsewhere. The light propagating in these fibres readily follows these bends with essentially no propagation loss.

However, optical fibres are finding more diverse application in an ever-increasing number of areas, such as sensing, security, aircraft, submarines, motorcars, computers, medicine, etc. In some of these applications, the fibres need to be bent to quite small radii of only a few centimetres or less. In this situation, it is much more difficult to contain the light within the fibre, as it tends to leak out of the side of the fibre when it cannot follow the rapid change of direction of the fibre's path. The resistance of fibres to this bend loss can be enhanced to some extent by a suitable design of the fibre's refractive index profile that provides tighter confinement of the light to the centre of the fibre.

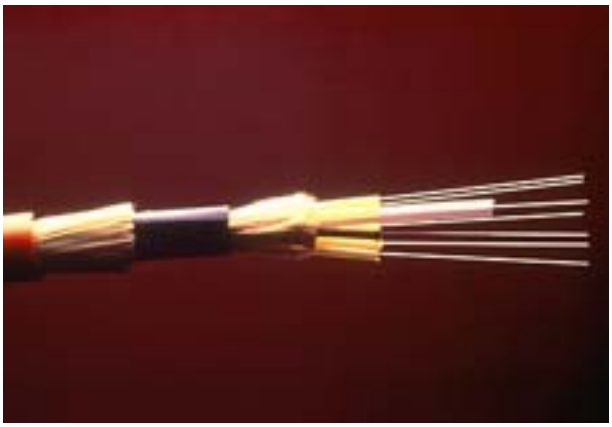

Optical cable cut back to reveal the fibres

The conventional qualitative explanation of fibre bend loss that has been extant for several decades treats it in terms of a superposition of transient losses that occurs at both the beginning and end of the bend, where the curvature changes very rapidly, together with a steady loss that continuously accumulates along a bend of constant radius, somewhat akin to the radiation from a bent antenna.

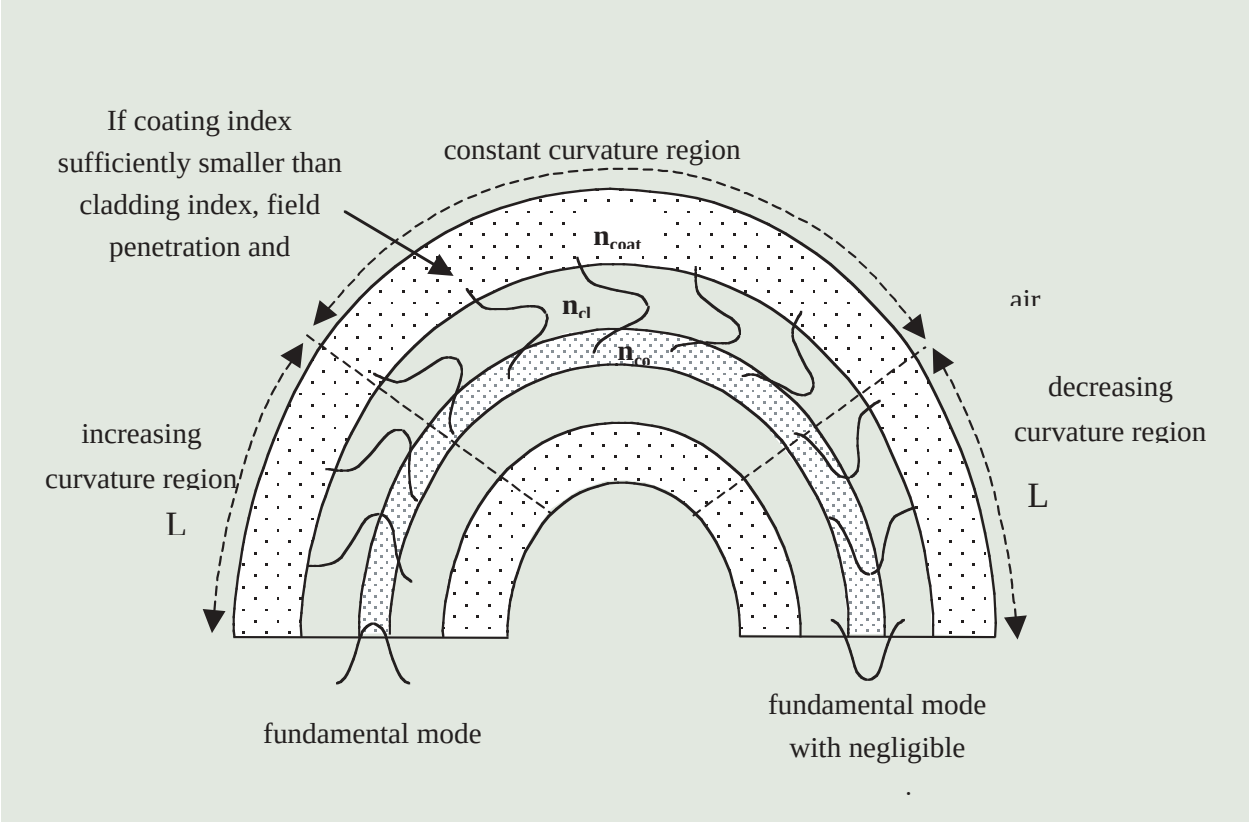

Evolution of the fundamental mode around a low-index cladding bend showing the path of the fundamental mode field.

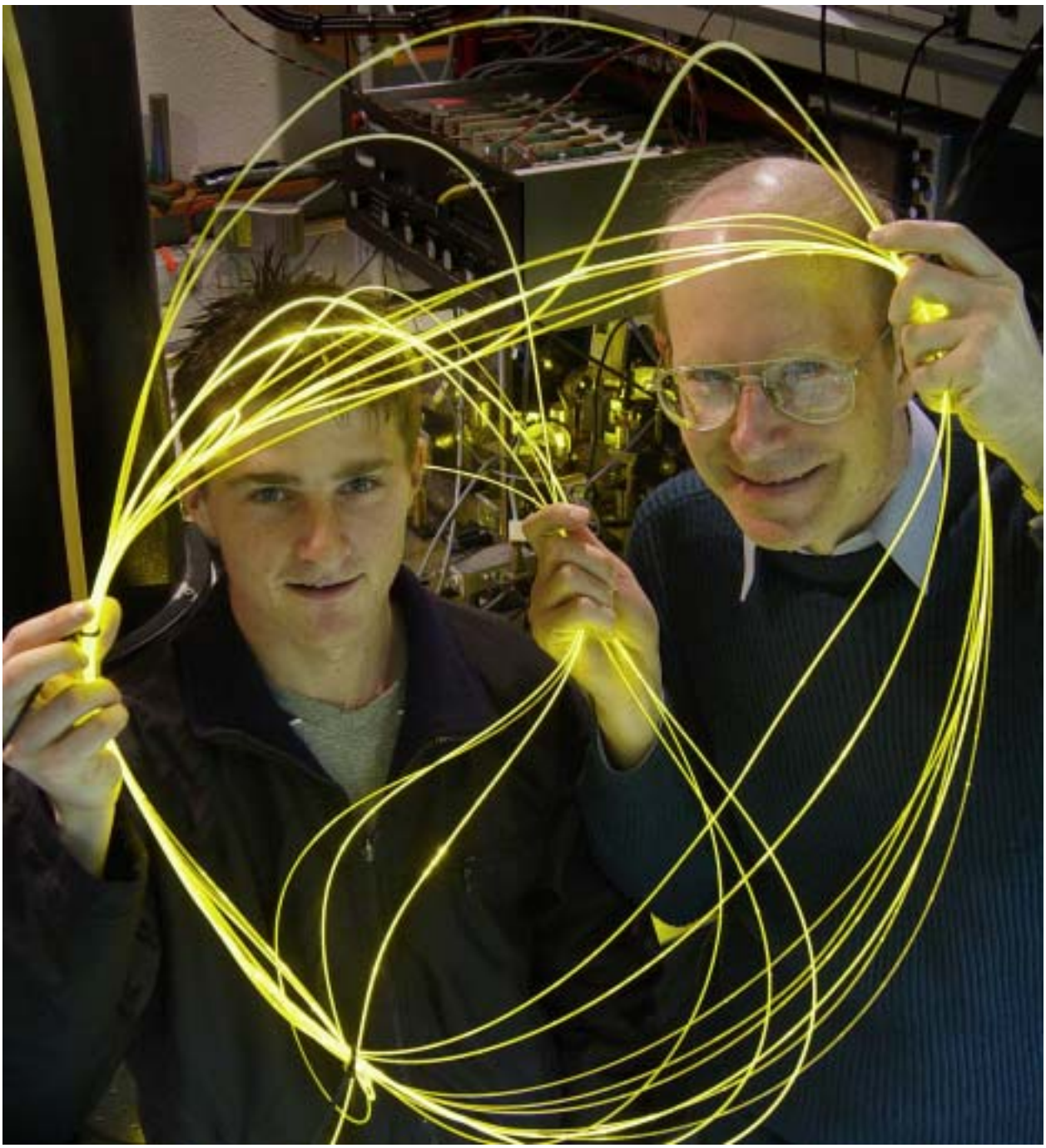

Adrian Ankiewicz and Andrew Molloy demonstrate light leakage from a very lossy fibre.

A more insightful description of how loss occurs qualitatively has now been developed. This approach examines the physical evolution of the fibre mode into, along and out of the bend, and takes into account the finite structure of the cross-section of a practical single-mode fibre. In this description, the light field of the mode, that is approximately Gaussian-shaped, is laterally displaced with increasing curvature in the plane of the bend, as shown in the figure. However, provided the rate of change of curvature along the path is everywhere sufficiently small, the mode loses negligible power regardless of how large the curvature (or how small the radius) eventually becomes, as it is more readily able to follow the changing path. A simple criterion has been devised to provide an approximate upper bound on the rate of change of the curvature that relates this change to the beat length between the mode and the radiation field along the fibre.

Another factor that can affect loss along a bend is the coating that surrounds a fibre. A coating on a fibre is necessary to protect the glass from environmental effects and to provide additional strength, as a bare fibre will readily snap. On a bend, the coating acts as another barrier to the light escaping and will help guide the light around the bend provided that the coating material is optically less dense than the glass it is protecting. Otherwise if the coating is denser than glass, light will be attracted into the coating and since the coating material is normally opaque, light will be absorbed there. Ironically, early fibre coatings used a silicone material with lower index, whereas contemporary coatings use a higher-index acrylic.

This new approach to understanding bend loss will help in the design of fibres, optical waveguides and light-processing devices where considerations such as compactness become an issue.

Leaky Modes in Luminescent Nanocrystal Waveguides

Rob Elliman, Nat Smith, Marc Spooner, Andrew Wilkinson and Tessica Weijers.

Silicon nanocrystals (Si-NCs) can be formed in fused silica substrates by the precipitation of excess silicon. Such nanocrystals exhibit efficient room temperature photoluminescence (PL) as a direct consequence of their nanometre size and their presence increases the local refractive index of silica, enabling the fabrication of an optical waveguide. The properties of such waveguides depend not only on the waveguide geometry but also on the size and concentration of the nanocrystals, as these can absorb and scatter light as it propagates in the waveguide. This study looked at the properties of nanocrystal-containing waveguides and specifically at optical guiding of the light emitted within the waveguide structure by the luminescent nanocrystals. Although this is an unusual situation, the reported properties were found to be a general feature of asymmetric slab waveguides that have high optical losses in the core region.

Slab waveguides with different excess silicon contents were formed in fused silica plates by implanting the surface with high energy silicon ions, a process that produces a skewed Gaussian distribution of excess silicon beneath the surface. These were then heated to form a buried layer of silicon nanocrystals. Measurements were performed by irradiating the nanocrystal layer with a laser and comparing the PL emission from the sample surface with that guided to the edge of the sample (see Fig. 1). The results are shown in Fig. 2.

Fig. 2 (left column) shows PL spectra from four waveguides, each with a different silicon content. The broad dotted curves represent PL from the sample surface while the other curves (continuous lines) represent PL collected from the edge of the sample. Clearly these spectra are very different. Typical PL spectra from silicon nanocrystals consist of a broad band centred at 700-800 nm, consistent with the dotted curves in Fig. 2. However, the edge emission is much narrower and contains (except for the $3x10^{17}$ cm^{-2} sample) narrow TE and TM modes clearly resolved with a linear polarisation filter parallel (TE) or perpendicular (TM) to the layer edge. The crucial question to be addressed is how do these narrow lines originate?

The "buried" nanocrystal waveguides have a refractive index profile, n(z), determined by the ion-implantation parameters. Such profiles were measured by fitting interference fringes in VIS-IR transmission spectra. These were found to have a maximum refractive index at a depth of d = 0.63 μm and to have asymmetric profiles, tailing towards the surface, consistent with the implanted silicon distribution. Using these profiles it was possible to model the optical properties of the waveguide. This showed that PL emitted at depth *d* at high enough angles θ undergo total internal reflection at the core-cladding interface and propagate within the nanocrystal core region as normal guided modes (representing a continuous spectrum). However, rays emerging at angles θ that are close but slightly below the critical angle for total reflection at the core-substrate interface can reach the sample surface z = 0 and be totally reflected at this boundary. This reflection introduces an extra step-like phase shift that causes the splitting of the TE and TM modes. The reflected beam then propagates through the core region and undergoes partial reflection from the core-substrate interface. At each such reflection a small fraction of the energy can leak from the core layer into the SiO_2 matrix as a substrate mode. This finally leaves the sample edge at an angle close to zero.

The results of such calculations are presented in Fig. 2 (right column). The overall agreement with the experimental data (left column) is excellent, providing strong support for the proposed model.

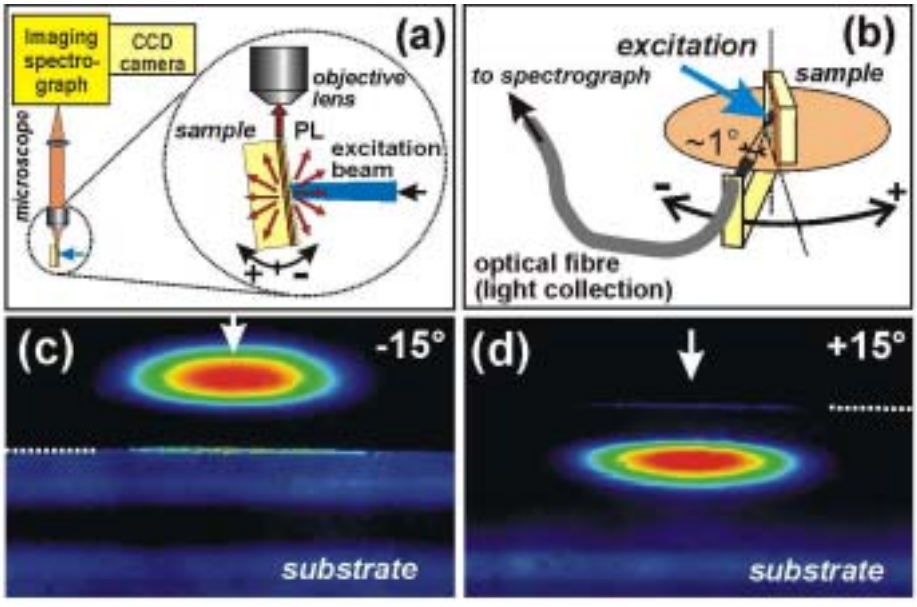

Fig. 1. Schematic of the experimental conditions employed for: a) micro-PL, and b)angle resolved measurements. Lower panels show PL images (area 2x1.2 mm^2) of the excited waveguide (using micro-PL set-up) for sample inclination of: (c) α=-15°, and (d) α=+15°. The elliptical spot is the excited region on the sample surface, and the narrow line is the guided PL emitted from the sample edge.

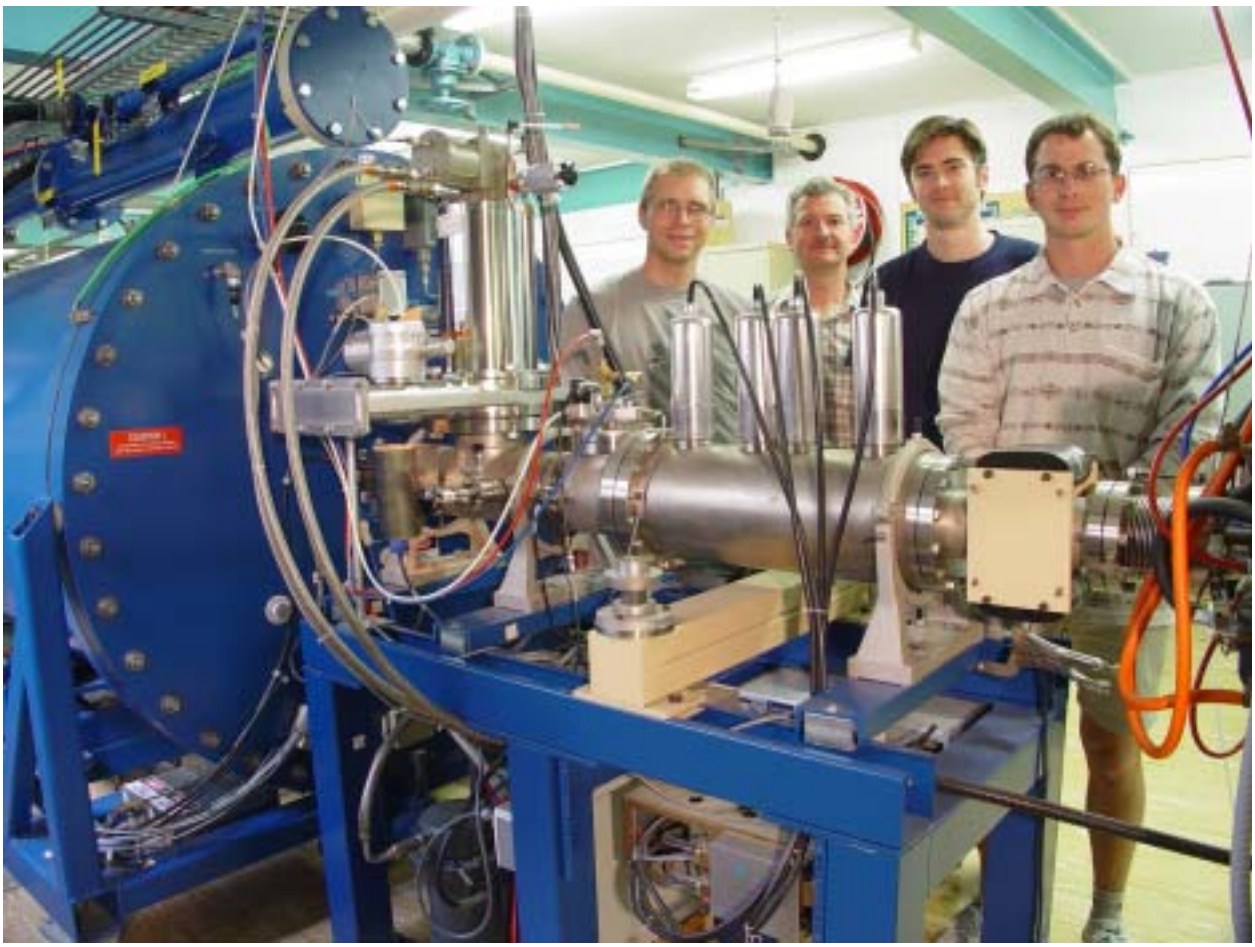

Marc Spooner, Rob Elliman, Andrew Wilkinson and Nat Smith with the high energy ion-implanter

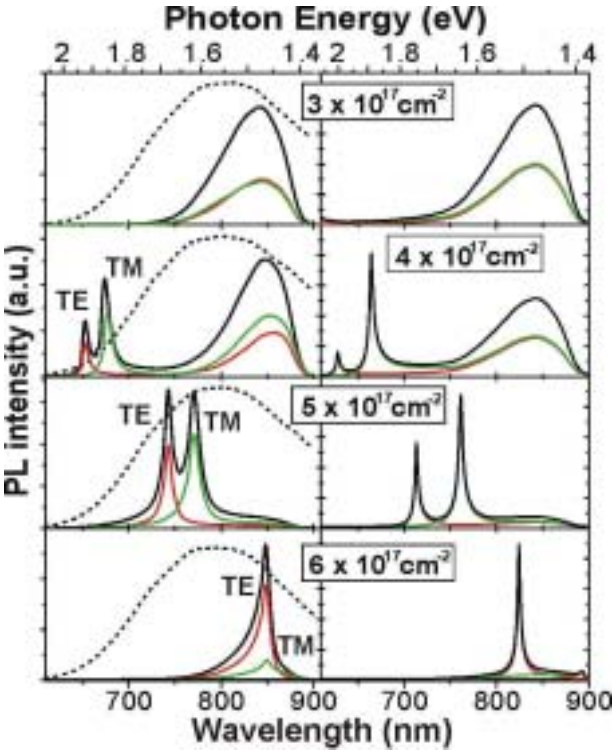

The question that remains is why the substrate modes are so significant here. A likely answer to this question is that the regular guided modes experience greater loss during their propagation in the plane of the waveguide. Indeed, the beams responsible for generating the substrate modes travel reduced distances through the core region and once launched, the substrate mode undergoes virtually no loss in travelling to the substrate edge. On the other hand, the standard guided modes are strongly damped as they pass through the nanocrystal layer, an effect that increases with increasing nanocrystal concentration. The model employed here does not depend on the nature of the core losses but simply on the fact that the loss is significant. As such, it is expected to be a general phenomenon for waveguides with high core losses.

(This work was undertaken in collaboration with: J. Valenta (Charles University, Czech Republic), T. Ostatnick (CNRS, France), I. Pelant Academy of Sciences, Czech Republic), P. Janda (Charles University, Czech Republic), J. Linnros (Royal Institute of Technology, Sweden), and B. Hönerlage (CNRS, France))

Fig. 2.Left column: Experimental PL spectra for layers implanted with doses 3, 4, 5, and 6 x10^{17} Si.cm^{-2} detected in two different directions: The conventional normal incidence PL spectra (dotted line) and PL spectra from the sample edge (black line - PL without polarizer, red line - with polarizer parallel to the layer (TE mode), green lines - polarizer perpendicular to the layer (TM mode)). Right column: Calculated PL spectra. (Black lines – the overall intensity, color lines – particular polarizations.)

ANU X-Ray Specs Render Your Bones Transparent

Mark Knackstedt, Tim Senden, Anna Carnerup, Arthur Davies and Tim Sawkins

A high resolution X-ray microscope with three-dimensional imaging capabilities has been designed and built in the Department of Applied Mathematics. More precisely termed X-ray micro-computed tomography (CT) the facility was designed to pursue research in the field of mesoscale physics. As a subject, it covers complexity, disorder, cooperative effects and structure-property relationships within length scales that lie in the sub-micron to millimetre range. Much of modern material science can be found in this regime and it remains a rich ground for new research. As many of the phenomena ascribed to this regime span several orders in length scale and are inherently three-dimensional (3D) in nature, the CT facility is a valuable addition to many research projects.

Tomography is a technique that generates 3D data sets, called tomograms, from a series of radiographs collected at dierent viewing angles. This series of radiographs is then computer reconstructed into a tomogram, which represents the internal structure and compositional variation of a specimen obviating the need to physically dissect that specimen. The instrument in this facility employs a highly focussed X-ray source and is designed

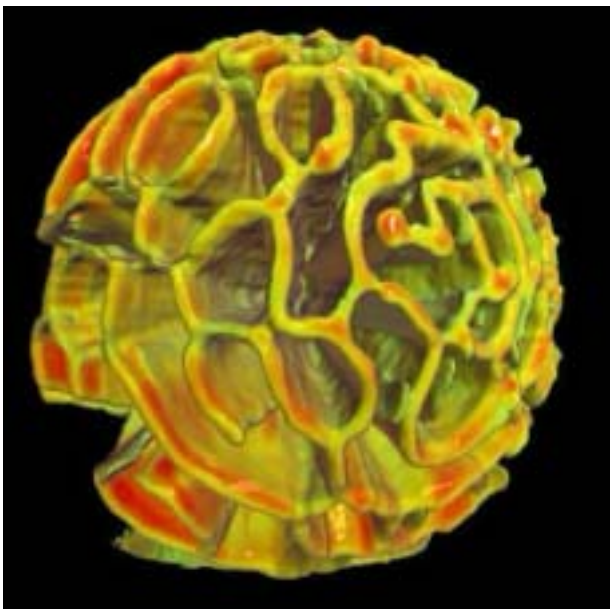

A barium/silicate biomorph

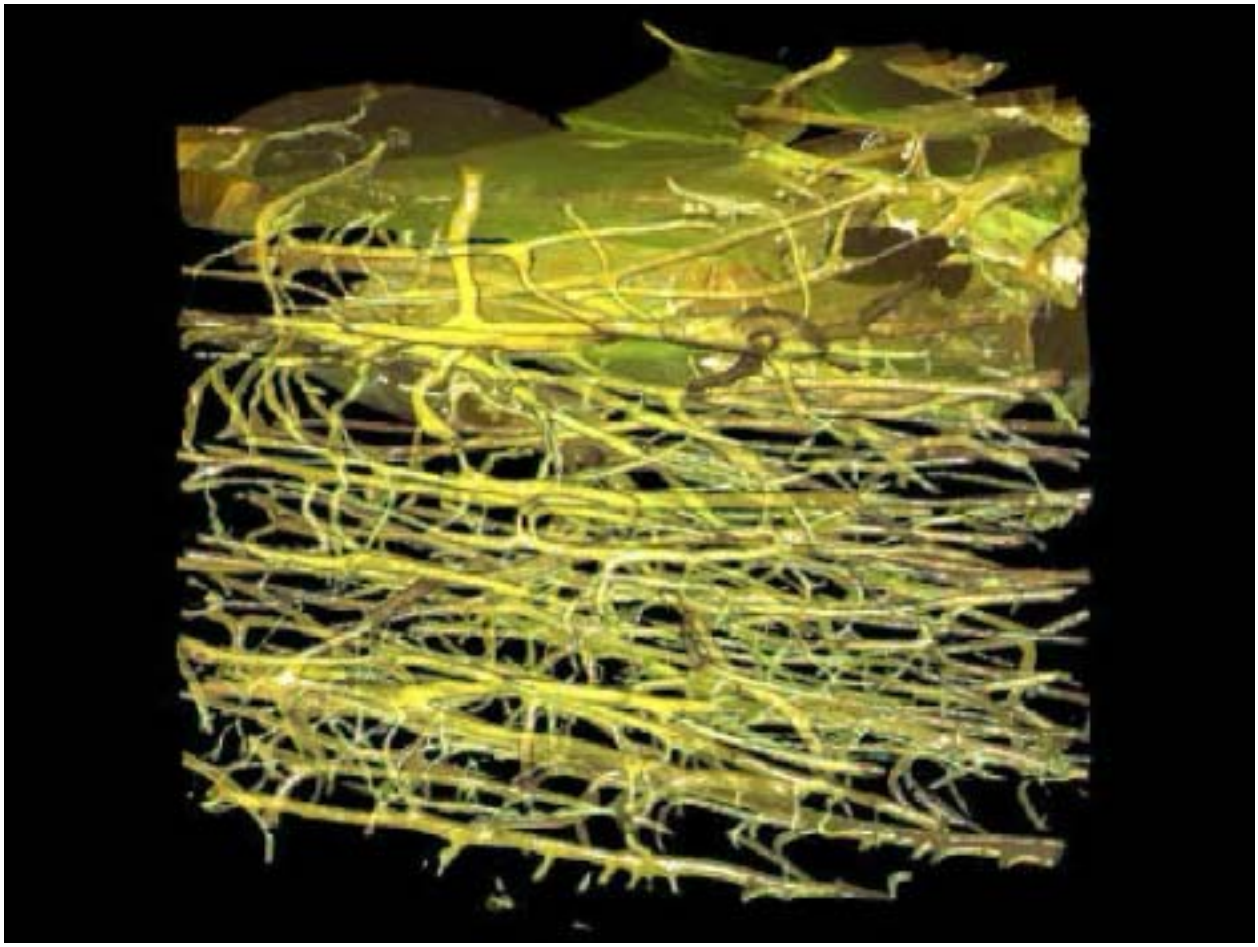

Human cortical bone showing Haversian and Volkmann canals

Members of the X-ray CT team with the facility

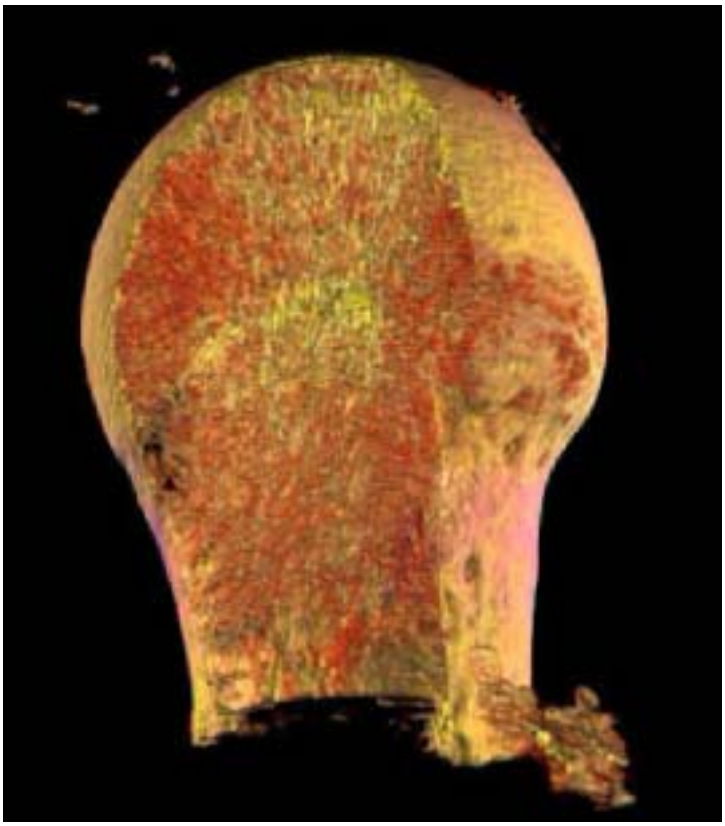

Fractured human femoral head

to have an extremely large field of view (20483 voxels (3D pixels) and high spatial resolution 2 m). Combining this high brilliance source with a large dynamic range detector the facility has ample versatility to develop various imaging techniques and sufficient throughput to permit slow time series experiments. Below, a photo of the instrument is shown. To date, the facility has collected and analysed 240 tomograms with 10243 voxels and 20 tomograms with 20483 voxels. This represents 1.3 TeraBytes of data which would have been impractical to generate and analyse if it were not for the generous support of the Australian Partnership for Advanced Computation. The types of specimens analysed include sedimentary rocks, soils, bone, soft tissue, ceramics, fibre-reinforced composites, foams, wood, paper and small animals. The task of data analysis occupies the large part of the groups' effort. Directly from the tomograms, properties such as fluid diusion and permeability, elastic and bulk moduli, sonic velocities, thermal conductivity, network and morphological analysis and dynamics are extracted. Below are some examples of the specimens analysed. The pictures are volume renderings generated from the 3D tomogram data and are all generated by Ajay Limaye at VizLab.

Nonlinear Photonics in Optically-Induced Lattices

Yuri S. Kivshar, Dragomir Neshev, Andrey A. Sukhorukov, Elena A. Ostrovskaya, Tristram J. Alexander, Wieslaw Krolikowski, and Brendan Hanna

Nonlinear propagation of waves in periodic media has long been a focus of strong interest. The physics of this phenomenon is common for a variety of systems, including excitations in biological molecules, electrons in solid-state matter, ultracold atoms in optical standing waves, and light waves in nonlinear media with periodic modulation of the refractive index. However only in optics, can effects associated with this phenomenon be directly observed and examined in close detail. A strong motivation for work in this area comes from the analogy between the behaviour of light in periodic photonic structures and electrons in superconductors. This analogy suggests the possibility of replacing electronic components with novel types of photonic devices where light propagation is fully controlled in engineered micro-structures. Nonlinearity adds a possibility to control propagation of light purely optically, i.e. with light itself. Such all-optical devices may form foundation of future high-bandwidth, ultrafast communications and computing technologies.

In practice, development of new schemes for controlling light in periodic structures is hindered by difficulties that arise in fabrication of materials that have both periodicity on the optical wavelength scale and strong nonlinearity accessible at low laser powers. In a joint effort between the Nonlinear Physics Centre and Laser Physics Centre, we circumvented these difficulties and implemented a "quick and simple" way to produce reconfigurable periodic structures with strong nonlinearity. We induce periodic modulation of the refractive index in a highly nonlinear photorefractive crystal by using a periodic interference pattern of several broad laser beams [Fig. 1] and employing a natural ability of the crystal to respond to light by changing its refractive index. The resulting periodic refractive index profile acts as a regular array of optical waveguides for any probe beam entering the crystal. Because this array is "written" by laser light, we call it an *optically-induced lattice*. Our experimental set-up (photo) allows for unprecedented flexibility and dynamical tunability of the optically-induced photonic lattices. The modulation depth of the refractive index is controlled by the external electric field applied to the crystal, lattice periodicity and dimensionality – by changing the geometry and number of interfering beams.

Periodic structure of the optical refractive index induces a band-gap structure of spectrum for the propagating optical waves. The existence of gaps implies that optical waves with certain wave-vectors cannot propagate through the structure due to either total internal, or Bragg reflection. The dynamics of any

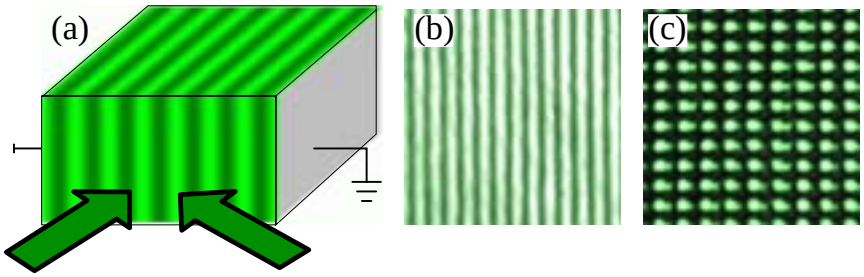

Fig. 1 (a) Schematics of one-dimensional lattice generation in a photorefractive crystal by using interference of two laser beams, and light intensity patterns formed by a (b) one- and (c) two-dimensional optical lattices on the crystal output face.

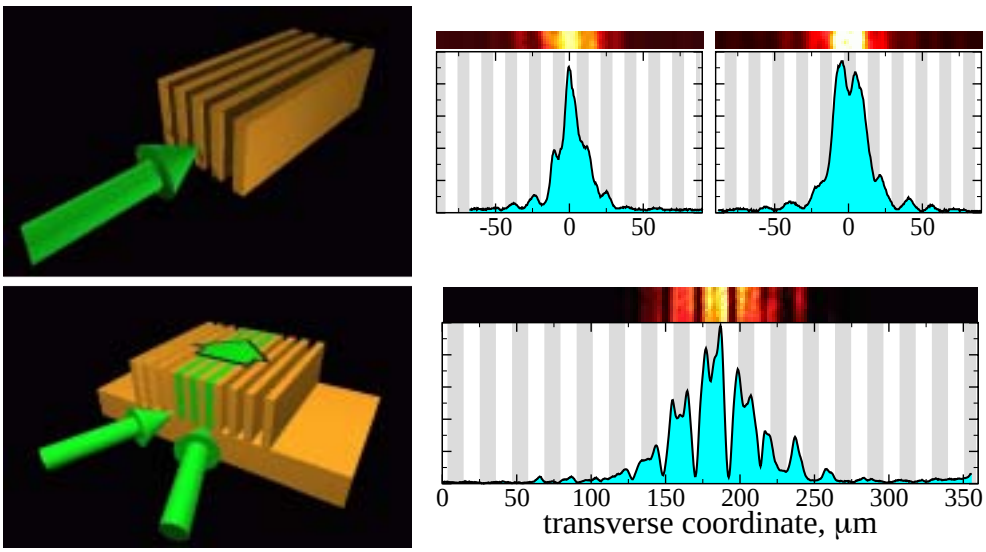

Fig. 2 Left: Excitation schemes for discrete solitons (top) inside a total internal reflection gap and gap solitons (bottom) in a Bragg reflection gap. Right: Experimental intensity profiles of two discrete solitons, centered on or between induced waveguides (top) and a gap soliton (bottom). Shaded areas show minima of the induced refractive index grating.

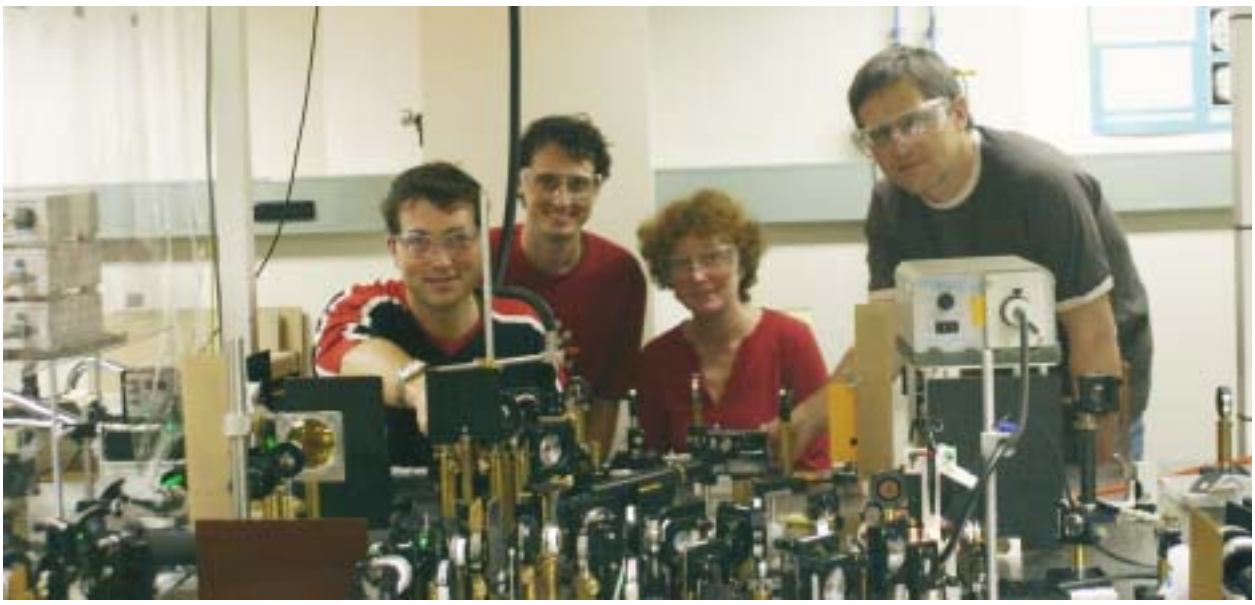

Dragomir Neshev, Tristram Alexander, Elena Ostrovskaya and Wieslaw Krolikowski with the expereimental setup for inducing photonic lattices.

probe laser beam propagation in a nonlinear optically-induced lattice is therefore dominated by an interplay between nonlinearity of the medium and scattering from the periodic structure. Our group conducts theoretical and experimental studies of the key aspects of light propagation in nonlinear photonic lattices, and recently we demonstrated a number of novel remarkable phenomena, including formation and steering of *discrete and gap solitons*, and trapping and stabilization of a *discrete vortex*.

Discrete lattice solitons are self-trapped, spatially localized and non-diffracting beams of light that, due to self-focusing nonlinearity of the crystal, can be trapped in the total internal reflection gap of the periodic structure. Their intensity profile is only slightly modulated by the lattice, and their excitation in the lattice is a threshold effect depending on the level of the input or laser power [Fig. 2]. In contrast, *gap solitons* are nonlinear beams that can be trapped inside Bragg reflection gaps of the optical lattice. Their excitation is non-trivial as it requires zero transverse velocity relative of the lattice and careful selection of the wave-vector corresponding to the particular spectral region inside the gap. Both requirements were satisfied in our successful (and first of its kind) experiment on generation of immobile gap solitons in one-dimensional optical lattices by using a twin-beam excitation scheme [Fig. 2]. In addition, this experiment confirmed our theoretical prediction of anomalous steering behaviour of gap solitons, which can be fully explored and exploited for the purpose of light control in optical lattices. Mobility and interaction properties of lattice solitons are strongly affected by the lattice, and are under our further investigation.

Two-dimensional optically induced lattices enabled us to study propagation and localization of beams with complex topological structure, such as optical vortices. Optical vortices are beams of light with quantized circulation of energy, carrying a phase singularity. The intensity of light at the vortex core is always zero, and in a nonlinear medium vortices can be spatially localized as vortex solitons [Fig. 3(a)]. Remarkably, vortex solitons "survive" in the lattice, where their intensity profile is strongly modulated, but a directional flow of energy is preserved [Fig. 3(b)]. We demonstrated the experimental generation of a *discrete vortex soliton* in a photorefractive crystal [last panel in Fig. 3]. Unlike the vortex propagating in a bulk self-focusing medium, where it quickly disintegrates, the discrete vortex is stabilized by the lattice. More recently, we discovered that lattices may support a novel class of asymmetric vortex solitons with no counterparts in homogeneous media [Fig. 3(c)]. Experimental observation of the broad class of asymmetric vortices in photonic lattices is underway.

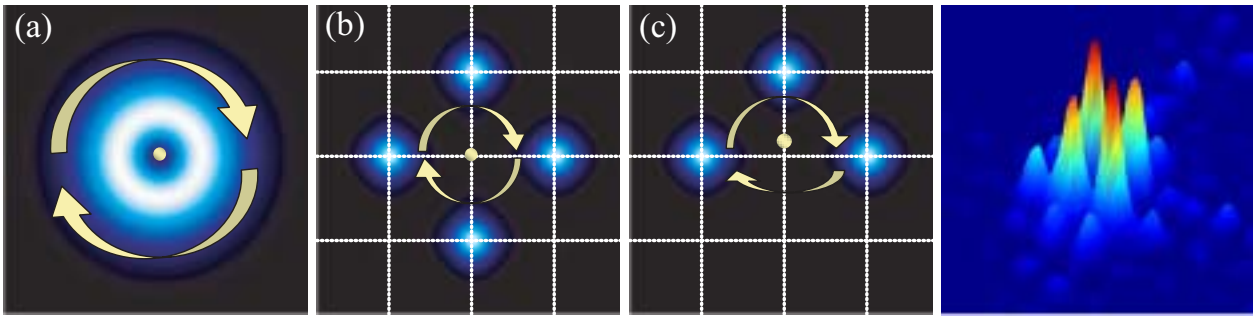

Fig. 3 Schematics of the light intensity distribution in an optical vortex soliton (a) in a bulk nonlinear crystal, (b) in a two-dimensional "square" photonic lattice. Arrows show the directions of the energy flow. Panel (c) shows a non-trivial asymmetric vortex predicted to exist in the spectral gaps. Last panel shows the characteristic four-peak intensity distribution of the discrete soliton in the total internal reflection gap, observed in our experiments.

The Missing Link

Anna Wilson, George Dracoulis, Aidan Byrne, Paul Davidson and Greg Lane

What is superdeformation?

It came as a major surprise when experiments in the mid-80s showed that some rapidly spinning nuclei can adopt extremely deformed shapes, rather like rugby balls, without splitting into two (fissioning) because of the associated stresses. These exotic nuclear states are stabilised by effects due to nuclear shell structure (analogous to the electronic shells in atoms) which give extra binding energy at large deformations. When nuclei take on such shapes they are described as superdeformed.

As can be seen in the figure, the excited superdeformed state occupies a real quantum well, separated from the ground state quantum well by a potential energy barrier. The problem of how the nucleus escapes from the superdeformed minimum is one with parallels in many fields - direct analogies can be made with the nuclear fusion process, or transport between coupled quantum dots. In fact, it is an example of the more general phenomenon of quantum tunnelling.

What is the missing link?

Unless we know the excitation energy of these states, it is impossible to extract detailed information concerning either their underlying structure or the mechanism which allows the escape from the superdeformed well to take place. Despite the fact that more than 100 superdeformed states have been identified in nuclei with mass numbers around 150 and 190, it has only been possible to measure their excitation energy precisely in four cases: ^{194}Pb, ^{194}Hg, ^{152}Dy and, in ANU-led work, ^{192}Pb. One of the reasons that it has proved difficult to make these measurements is that, for every superdeformed nucleus that we make in a fusion reaction, we make hundreds of others in other states. Even worse, when we do make a superdeformed nucleus, it can decay out of the superdeformed well and down to the nuclear ground-state by any one of thousands of different paths. If we want to measure the excitation energy, we must be able to trace one or more of these paths - that is, we have to find the missing link between the superdeformed and ground states. Because of this, it is essential that we apply the most efficient data selection methods possible.

Time-correlations the key to the search

The Gamma-ray Spectroscopy Group in the Department of Nuclear Physics has pioneered a technique which turns out to be ideally suited to filtering the data for certain superdeformed nuclei. The method exploits the fact that some special excited nuclear states survive for much longer than most others. These "isomers," which are less excited states where the nucleus has a normal shape, persist for fractions of a microsecond (a millionth of a second) before decaying down to the ground state. In contrast, typical lifetimes of superdeformed states are less than a picosecond (a million millionth of a second). Using modern fast-timing techniques, it is posible to correlate decays that feed the isomers with decays that follow them. This is a powerful selection tool: by selecting the subset of the nuclear levels whose decays feed an isomer, we throw away an otherwise overwhelming background of unwanted information.

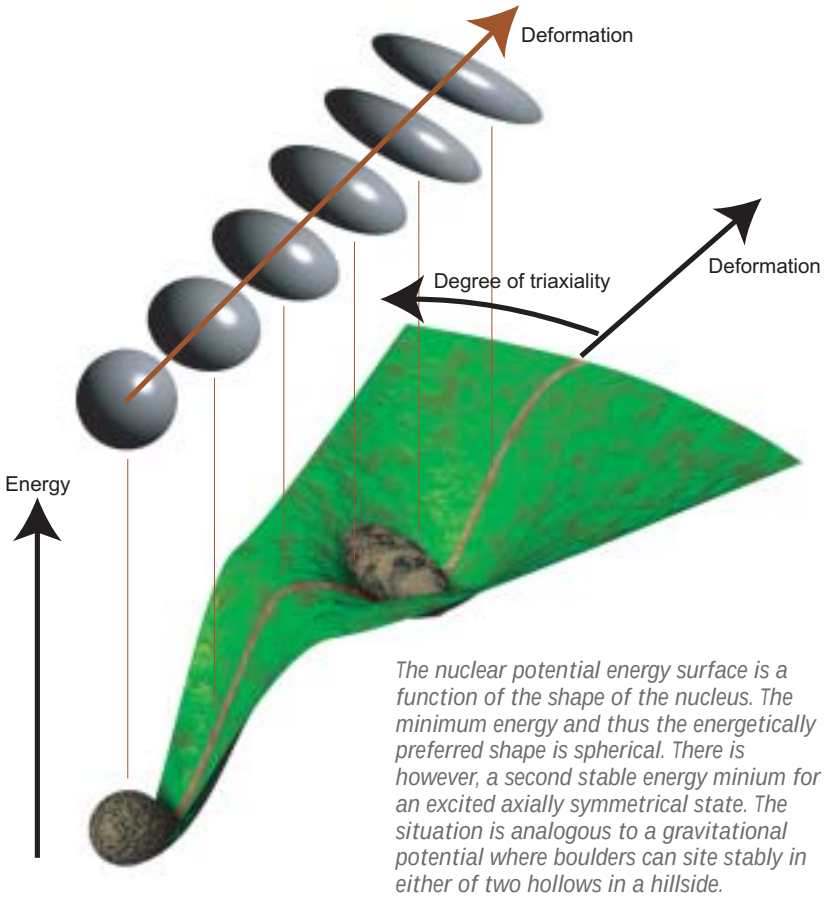

The nuclear potential energy surface is a function of the shape of the nucleus. The minimum energy and thus the energetically preferred shape is spherical. There is however, a second stable energy minium for an excited axially symmetrical state. The situation is analogous to a gravitational potential where boulders can site stably in either of two hollows in a hillside.

Successful measurement using state-of-the-art equipment

While the facilities at the ANU are ideal for the essential step of accurately characterising the long-lived nuclear states, a more efficient detection system is required to detect the extremely weak gamma-ray transitions which are the object of the search. The ANU team, led by Anna Wilson, won approval for access to the Gammasphere array at Lawrence Berkeley National Laboratory in California to apply their technique to the nucleus ^{192}Pb in collaboration with USA groups and others. During the experiment, around 100 Gigabytes of energy and time data were collected over a period of about three days, as hundreds of billions of ^{192}Pb nuclei were created in reactions between a silicon beam and an erbium target. Without the time-correlation filter, it proved impossible to identify the missing linking transitions which connect the superdeformed and ground-state minima. But when the filter

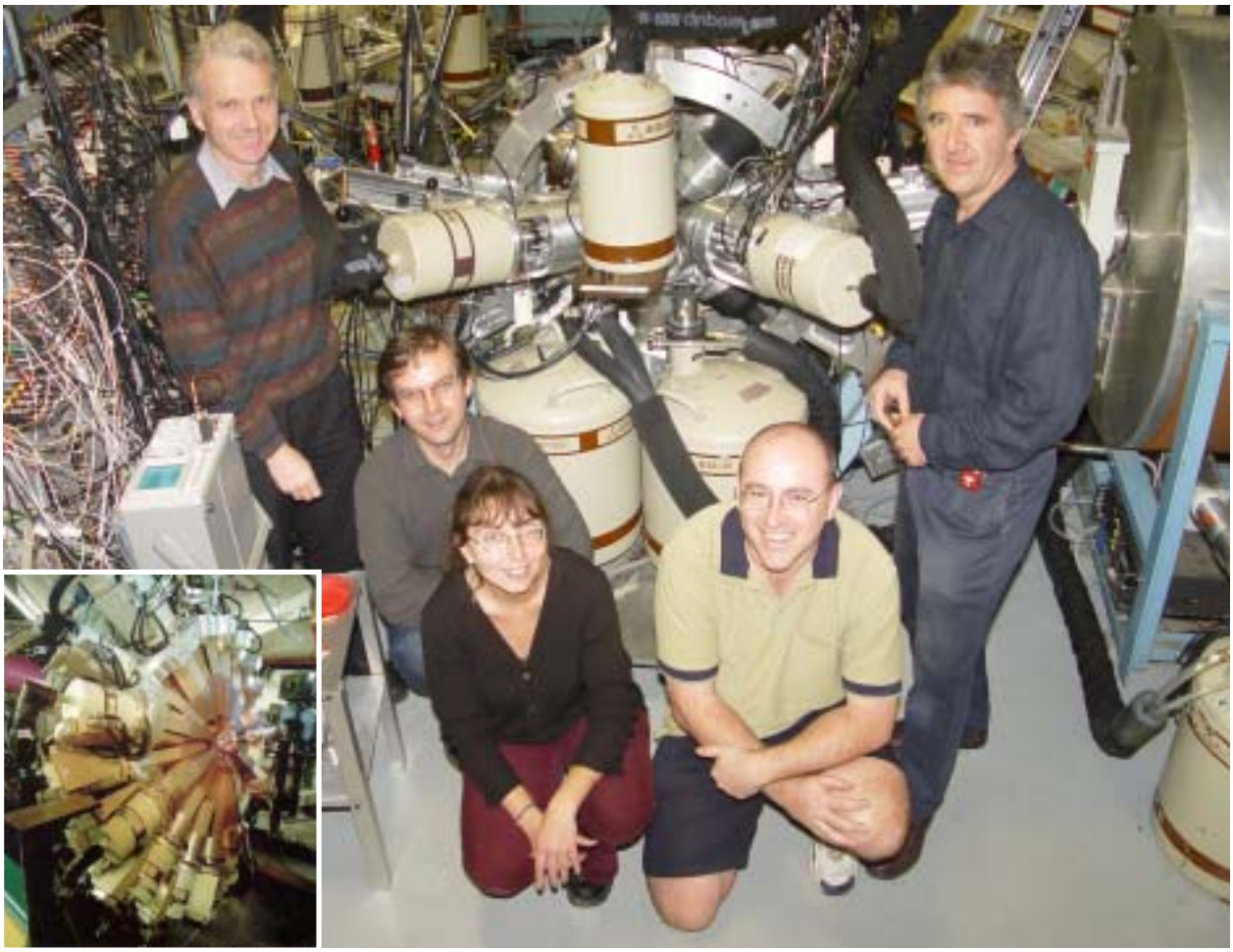

Researchers with the ANU gamma detector and insert: the gammasphere in the USA used to collect this data

was applied, the extra selectivity provided meant that some linking transitions stood out clearly above the drastically-reduced background.

The Gammasphere measurement established the excitation energy of the superdeformed well in ^{192}Pb as only about 2 MeV. This is extremely low, and has important implications for current theories of the tunnelling process between superdeformed and ground-state minima. The results have already prompted new theoretical investigations into the problem of the decay out of the superdeformed minimum.

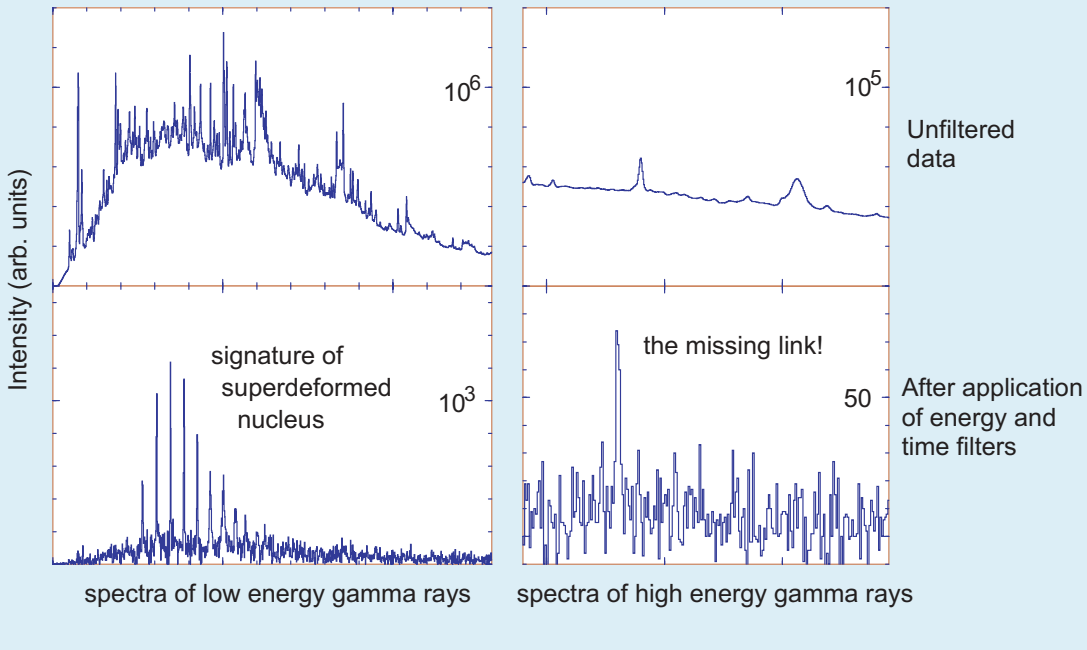

Plasma Turbulence Self-Organisation in H-1Heliac

Michael Shats, Horst Punzmann, Hua Xia and Marko Alat

New results from the H-1 Heliac at the Plasma Research Laboratory suggest that the plasma turbulence in toroidal magnetic fields self-organises into large structures. This makes plasma turbulence somewhat similar to the two-dimensional (2D) fluid turbulence observed, for example in planetary atmospheres and oceans. Though intuitively perceived as a more chaotic state (e.g., turbulent versus laminar flows), the 2D turbulence often shows a tendency to *self-organise* leading to a higher degree of order.

Well-known examples of the 2D turbulent structures in nature include large-scale vortices in oceans and atmospheres, such as the Great Red Spot of Jupiter, Gulf Stream rings, sunspots, Karman vortices formed in the flow past a solid obstacle and others. Among the biggest structures, which occur naturally in geophysical fluids, are *zonal flows*. Familiar examples of zonal flows include West-East winds in Earth's atmosphere, Jupiter's zonal flows, a rapid rotation of the Venusian's atmosphere (60 times faster that the planet itself), large-scale oceanic and atmospheric jets etc. Zonal flows are anisotropic, "zonally" localized flows generated by turbulence.

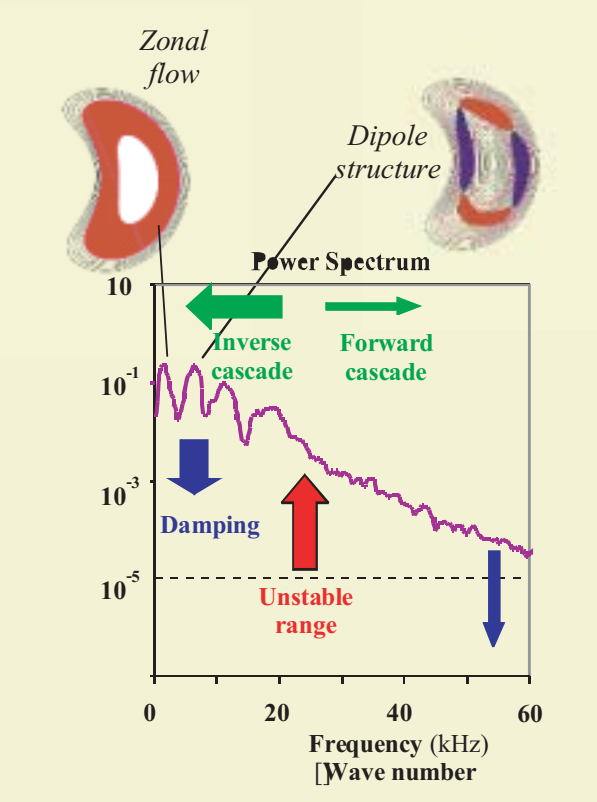

Fig.1. Flow chart of the energy flow within the turbulent spectrum. Inverse energy cascade leads to generation of large structures.

Jupiter's red spot (Courtesy NASA/JPL-Caltech)

The role and mechanisms of generation of large structures in plasmas are of fundamental importance to plasma physicists. Plasma turbulence has long been a prime suspect for the anomalously high loss of particles and energy across confining magnetic fields. The larger the turbulent structures the higher the effective diffusion of particles they cause. Understanding plasma turbulence is a crucial step towards control of plasma confinement in the future plasma fusion reactors, such as tokamaks and stellarators.

The process in which turbulent vortices merge together faster than they break up into smaller structures is called the *inverse energy cascade*. This effect has been theoretically predicted for plasma back in 1978 by A. Hasegawa and others and confirmed later by plasma computer modeling. In 2003 the first experimental evidence of the large structure generation due to the inverse cascade has been presented using data from the H-1 Heliac. The central part of this work is the computation of the energy, exchanged between vortices of different scales within the

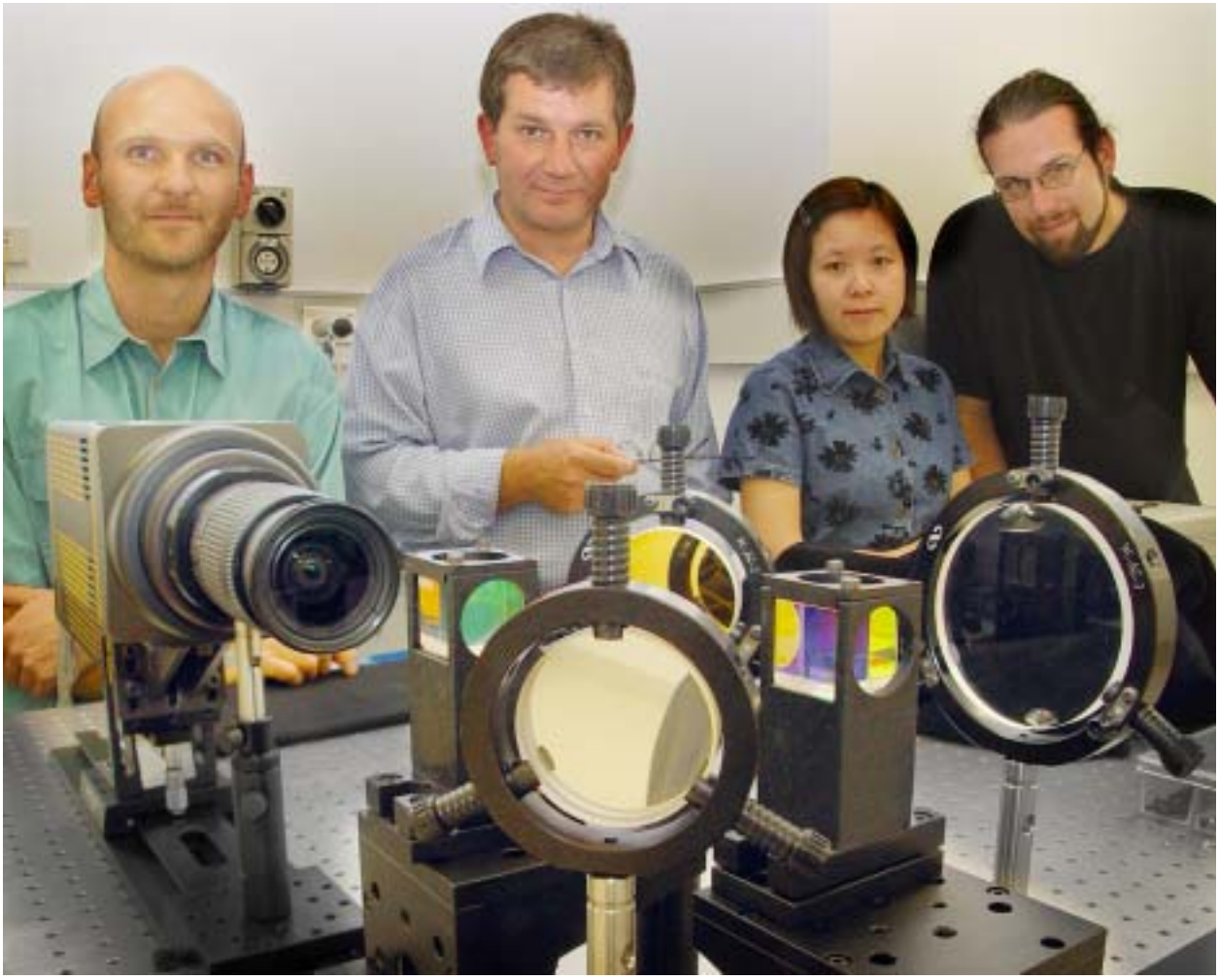

Horst Punzmann, Michael Shats, Hua Xia and Marko Alat with plasma imaging setup.

turbulent spectrum. Theoretical models adequately describe only special cases, not commonly found in large plasma experiments. In our experiments we deliberately produced plasma in which major theoretical assumptions were satisfied. This resulted in the first demonstration of the inverse cascade driving the generation of large structures, such as vortices and zonal flows as shown in figure1. Zonal flows have also been observed for the first time in the H-1 heliac. Now we have confirmed that the wave-wave interaction is the main mechanism of the zonal flow formation.

The inverse cascade is responsible for transferring spectral energy from the initially unstable spectral region (small-scale fluctuations) towards larger scale fluctuations, the most important region from the plasma action point of view. Large turbulent structures strongly interact with each other. We have discovered that zonal flows can modify properties of other structures in the plasma and can also dramatically change particle diffusion in the plasma. Particle fluxes across magnetic field are reduced in the presence of zonal flows while the turbulence level remain strong.

These discoveries have opened a unique opportunity to study self-organisation in the open energy systems (of which plasma is a good example) in the well-controlled laboratory conditions of the Heliac, using techniques and diagnostic tools not applicable to other systems, for example, to extraterrestrial turbulence. Plasma self-organisation manifests also during "sudden" confinement jumps, the "low-to-high transitions", which lead to even higher degree of order, where turbulence is suppressed and the diffusion is further reduced. Such transitions are observed in the heliac plasma (Figure 2). Details of the physical mechanisms behind them may reveal a key to the plasma control.

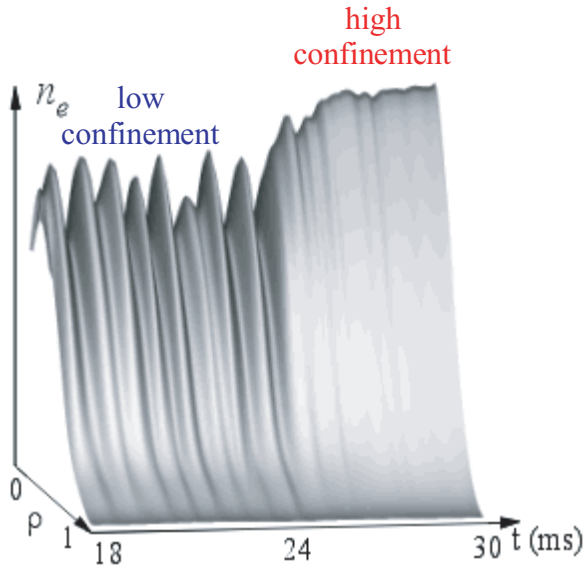

Fig.2. Time evolution of the plasma density during confinement bifurcation from low to high mode. The higher order in the plasma correlates with the turbulence suppression.

Exact Results for the Physics of Strong Coupling Ladder Compounds

Murray Batchelor, Xi-Wen Guan and Norman Oelkers

The ultimate challenge for theoretical physics is comparison with experiment. Yet often the development of theory is a fascinating and worthwhile endeavor in its own right. Over the past 40 years the theory of integrable models in statistical mechanics has developed to an extraordinary level of mathematical sophistication. By integrable it is meant that the eigenspectrum of the relevant Hamiltonian can be derived exactly. An essential ingredient is the Yang-Baxter equation, the so-called master-key to integrability. Recent progress has seen the development of a new approach to calculate the free energy of integrable models in terms of nonlinear integral equations. In 2002 Shiroishi and Takahashi solved the nonlinear integral equations using an exact high temperature expansion method to obtain the free energy of the spin-1/2 Heisenberg chain. Building on this approach, Batchelor, Guan, Oelkers and collaborators obtained the free energy of a spin-1/2 Heisenberg ladder model. This has led to comparison with experimental results for the strong coupling ladder compounds. The experimental realisation of compounds with a ladderlike structure has contributed to the intense interest in low-dimensional quantum systems. The existence of a spin gap, magnetisation plateaux, quantum critical points and superconductivity under hole doping are examples of key physical properties observed in the ladder compounds. The calculation of properties such as the full temperature phase diagram, the high field magnetisation curve and the specific heat have provided a significant challenge. These quantities have been obtained for the integrable ladder model using the exact high temperatute expansion (HTE) method. The figure below shows a comparison between the experimental (EXP) and theoretical results for the susceptibility as a function of temperature for the compound Cu_2(C_5 H_12 N_2)_2 Cl_4. The inset shows the magnetisation vs magnetic field for different temperatures. The critical magnetic fields H_c1 ~ 7.8 Tesla and H_c2 ~ 13.0 Telsa are also in good agreement with the experimental results. Also shown is the specific heat vs temperature for different values of the magnetic field. The inset shows the field dependent entropy vs temperature. The excellent agreement between theory and experiment is also seen for other known ladder compounds. The research reported here brings over 40 years of mathematical development into direct contact with experiment. Indeed, there is a strong expectation that integrable models will play a crucial role in understanding low-dimensional quantum effects, where they are most pronounced.

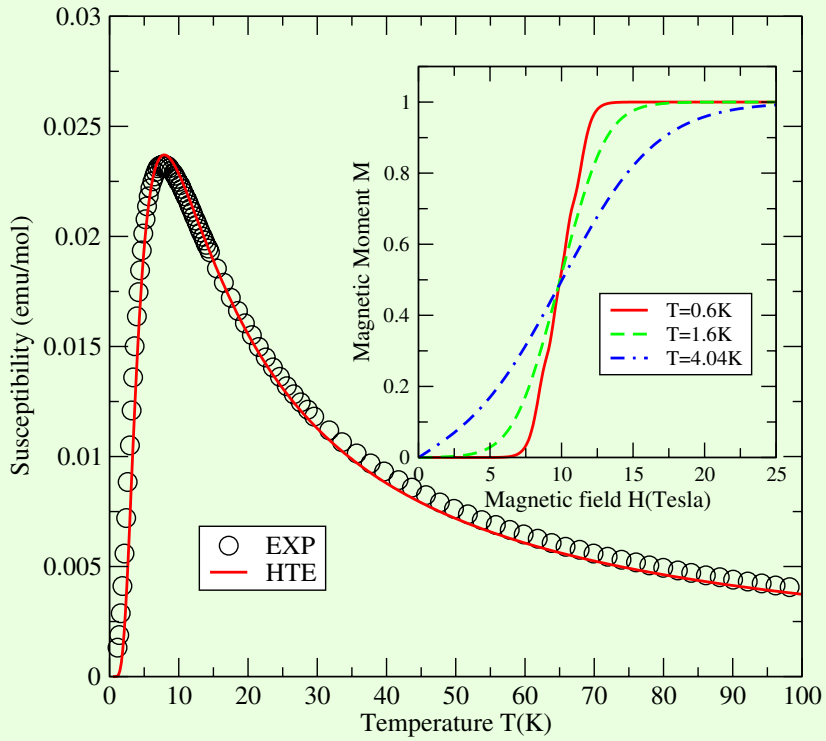

Comparison of theoretical and experimental results for the susceptibility and magnetisation.

Murray Batchelor, Xi-Wen Guan and Norman Oelkers tackle the mathematics of ladder compounds

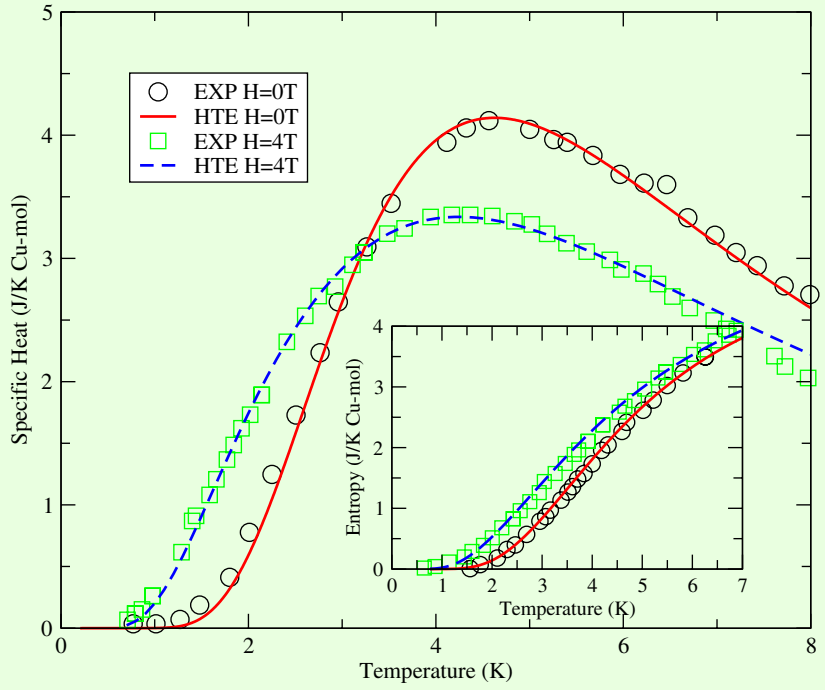

Comparison of theoretical and experimental results for the specific heat and entropy.

Velocity-map Imaging of Photoelectrons

Steve Gibson and Steven Cavanagh

In the course of developing a new apparatus for the study of dissociation, or fragmentation, of neutral molecules, it was realised that an innovative modification would also allow the probing of the intermediate zone between reagents and products of chemical reactions. This innovation has been made possible by an adaptation of an ion-imaging technique to image electrons. The significance of this new technique was recognised by the Australian Research Council which has funded the Discovery Project "Reaction transition states of halide-cluster complexes via velocity-map imaging of photoelectrons".

The initial thrust of the project was solely to investigate the fragmentation, or break up, of neutral molecules after their exposure to visible and UV light. When molecules are irradiated with photons, or light, of sufficient energy, chemical bonds can be broken causing of the original molecule to fragment. Information gleaned on how this light interacts with the original molecule, what fragments are produced and how it affects the fragments, can then be applied to problems of atmospheric, astrophysical and even industrial interest. In order to conduct such investigations a new experimental apparatus has been constructed, the fast-beam photo-fragment spectrometer, Fig.1, which is unique within Australia and one of only three worldwide. Detection of neutral atoms or molecules without the further use of light requires that the original molecules be given sufficient kinetic energy to cause a perturbation in the detector that is large enough to be detected using standard electronic means. In order to give the molecules this extra energy, they are first produced as a negative ion precursor. While existing as a negative ion the targets can be accelerated and focussed by electric fields.

Once the negative ion has been given enough kinetic energy the extra electron is removed by using a laser, leaving a fast moving neutral molecule, the subsequent fragments of which are capable of perturbing a detector enough so as to be detected.

However, the extra electron that is removed to produce the neutral species carries away with it information about not only the negative ion, but also the subsequent neutral species. Applying traditional electron detection techniques to a fast beam of negative ions is extremely difficult for a multitude of reasons. After a fortuitous set of circumstances it was realised that these difficulties could be overcome with the re-orientation and re-engineering of an existing electrostatic technique, pioneered by Eppink and Parker (U. of Nijmegen), called velocity-map imaging. The properties of this electrostatic lens is that for a given starting volume, each photo-detached electron from the negative ion with the same initial momentum will be mapped on to the same position on a two dimensional charged particle detector (see A in Fig. 1.). This physical mapping allows the extraction of the original electron velocities at the source.

The technique of velocity-map imaging of the electrons offers a number of significant advantages, including very high energy resolution (a few meV for 1 eV ejected electrons), the complete angular distribution of the ejected electrons and (since, the method is fully spatial) there is no requirement for short-pulsed lasers or fast electronic equipment. Preliminary measurements have been undertaken, using a prototype velocity-map imaging lens, which verify the technique. The accumulated detector image for the molecular oxygen anion (O_2^-) are shown in Fig. 2. The

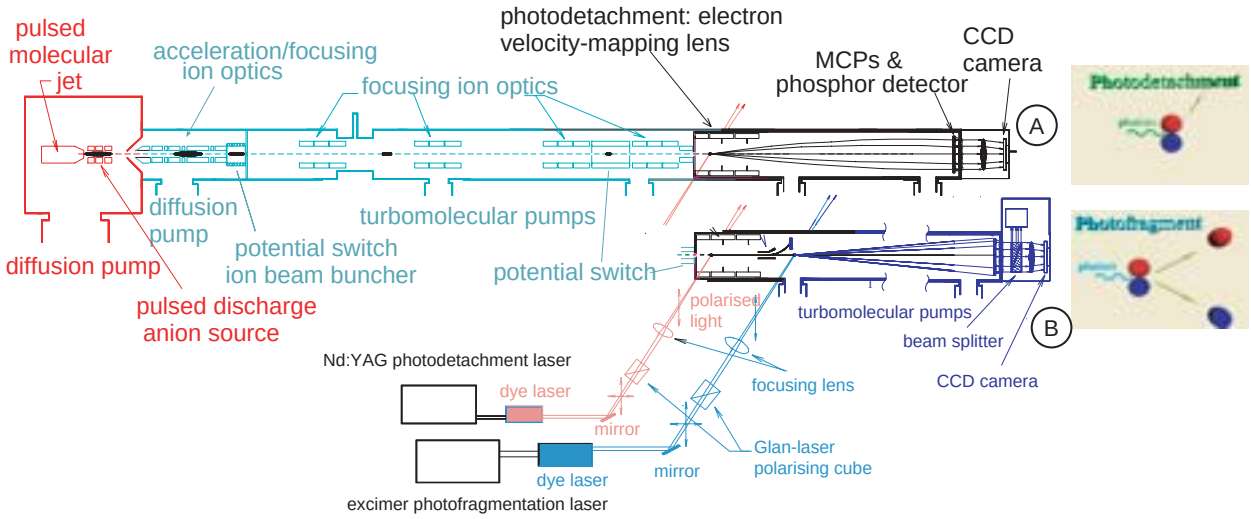

The ANU's fast-beam photofragment spectrometer which measures the breakup of a molecular species following its exposure to light. A fast moving molecular beam is produced by accelerating negative ions from a pulsed-jet/highvoltage discharge (far left), mass separating the ions and a laser beam removes the negative charge. A second laser beam breaks the molecule apart, producing fragments that are recorded by an imaging detector Ⓑ. The innovative inclusion of a velocity-map imaging lens at the first laser interaction region, provides a technique to analyse the detached electrons with unprecedented energy resolution Ⓐ.

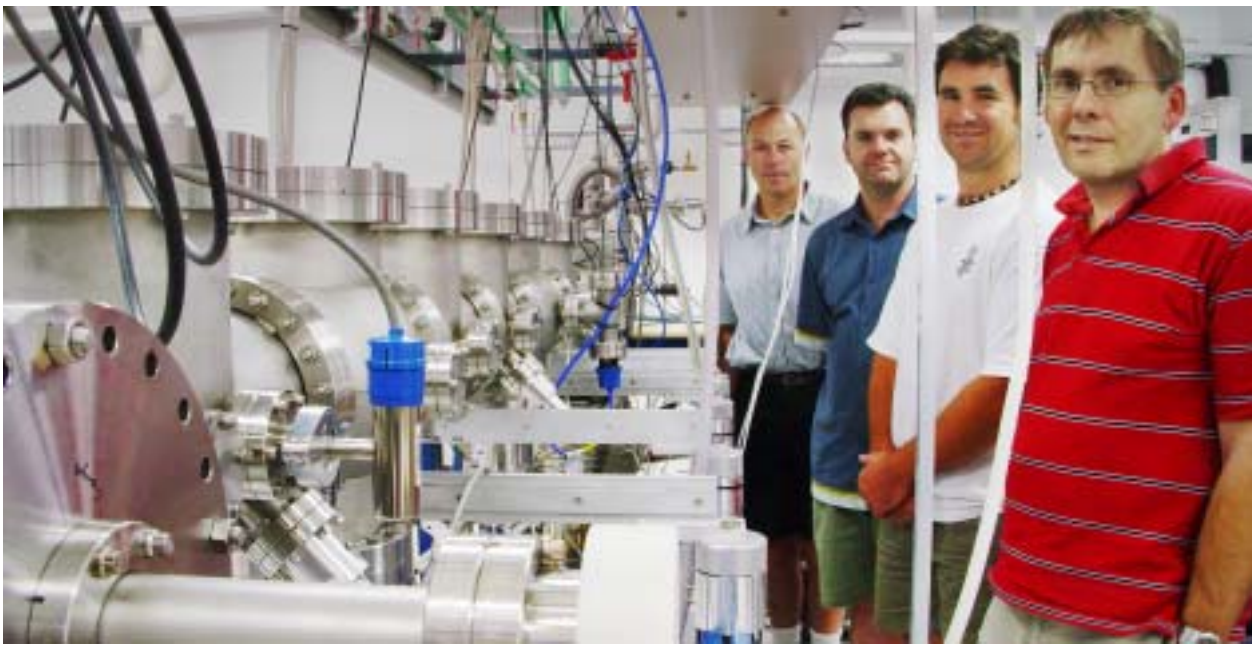

Steve Gibson, Steven Cavanagh, Garry Picker and Ed Roberts, alongside the fast-beam photofragment spectrometer

concentric circles correspond to the quantised energies for the ejected electrons, reflecting the energy structure of the oxygen molecule. Significant detail is available even from the test lens system, as revealed in the analysed image Fig. 3. An improved velocity-map imaging lens is to be installed early in 2004, which our computer simulations indicate will provide world-beating electron energy resolution.

The full benefit of our velocity-map imaging modification to the photofragment spectrometer comes from a strange quirk of photodetachment, that for some molecular species only the negative ion exists, with the neutral molecule breaking apart if the negative charge is lost. The corresponding neutral species may represent an intermediate state of a chemical reaction (ABC),

$$A+BC \leftrightarrow ABC \leftrightarrow AB + C,$$

that is present for a short period of time, called a transition state. The transition state controls the rate of a reaction and is very difficult to study due to its short lifetime during the course of a chemical reaction. The photodetachment process provides a method to access the transition state directly, see Fig. 4. Direct observation of the transition state has been acknowledged, by John Polanyi and Ahmed Zewail (both recipients of the Nobel Prize in Chemistry), as one of the "Holy Grails" of chemistry. An example of a transition state that is suitable for study in this way is an important class of halide-cluster complexes, such as H_2Cl, which form a set of prototypical reactions. These species also play important roles ranging from ozone depeletion through to industrial chemistry.

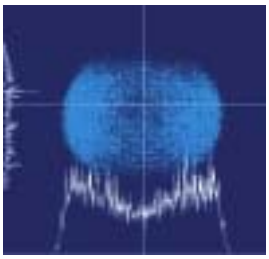

Figure 2: Velocity-map image of electrons detached from O_2^-. The image is an accumulation of many laser shots. Concentric rings reflect the discreteness of the electron energies. Horizontal and vertical slices through the image are also shown.

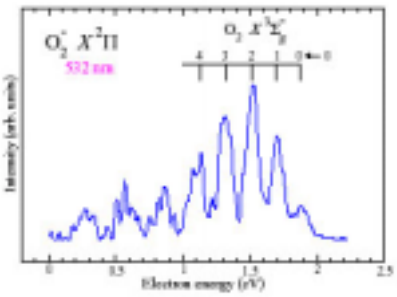

Figure 3: Analysis of the velocity-map image, qualitatively similar to unpeeling an onion, reveals electron energy structure corresponding to various energy states of the O_2^- molecule.

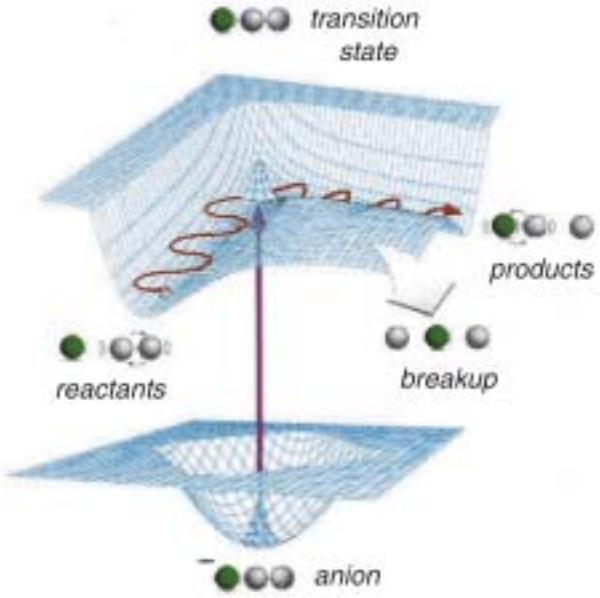

Figure 4: Potential energy surfaces for a stable negative ion (bottom) and the associated neutral molecular species (upper), illustrating the minimum energy reaction path and a barrier, the transition state, that controls the reaction rate. Photodetachment accesses part of the reaction path immediately above the anion energy minimum.

Electron Driven Processes in the Earth's Aurorae

Steve Buckman and Milica Jelasavicic

The spectacular shows of the Earth's aurora are driven by processes that occur in the rarefied atmosphere, 120 km above the earth. Here, in the ionosphere, interactions between electrons, ions, atoms and molecules lead to excitations of molecules, which then produce the colourful displays of light as they de-excite.

The nitric oxide (NO) molecule is only a minor constituent of the Earth's upper atmosphere. Nevertheless, it plays a major role in infrared auroral emissions due to radiation from vibrationally excited (NO*) states. Chemiluminescence, whereby excited nitrogen atoms interact with oxygen molecules to form vibrationally excited nitric oxide (NO*) and atomic oxygen, was long thought to be the main process leading to the formation of these excited molecules. Recent experiments within the Electron Physics Group indicate, however, that a different production mechanism for NO*, that due to excitation of NO molecules by low energy electron impact, is responsible for more than 20% of the NO auroral emission in the infrared.

A significant number of everyday processes, particularly those based on discharge technology and atmospheric/astrophysical phenomena, are driven by electron-molecule impact. In many cases, the nature of this interaction is profoundly dependent on the formation of intermediate, transient negative ion species which greatly enhance the reaction probability. Our experiments have shown that this resonant phenomenon is exhibited in collisions between low-energy electrons and nitric oxide, and have quantified the dominant role that NO- plays as an intermediary in the formation of vibrationally excited NO molecules. This negative ion complex lives for only 10-100 femtoseconds (10-15 s) and decays by losing its extra electron, preferentially leaving the molecule in a vibrationally excited level. Our measurements indicate that at low electron energies (1-3 eV), the vibrational excitation cross sections are enhanced by several orders of magnitude by the influence of the intermediate negative ion complex. When these new experimental data are included in existing atmospheric models of infrared auroral emissions, a new insight into the role of electron-driven processes in our upper atmosphere emerges.

Sophisticated computational packages have been developed in order to model and interpret these complex auroral phenomena, but with only modest success to date. These models depend, however, on the input of interaction probabilities, and as our work has shown, these are not always well-defined. Consequently, our colleagues at Flinders University have developed a suite of enhanced statistical equilibrium codes, which in conjunction with the new NO vibrational excitation probabilities determined by our recent studies, model the production mechanisms for vibrationally excited NO under auroral conditions.

The model was run using two different sets of interaction probabilities (cross sections) to describe the electron-NO interactions. The first set (CSS1) is that used in the earlier study

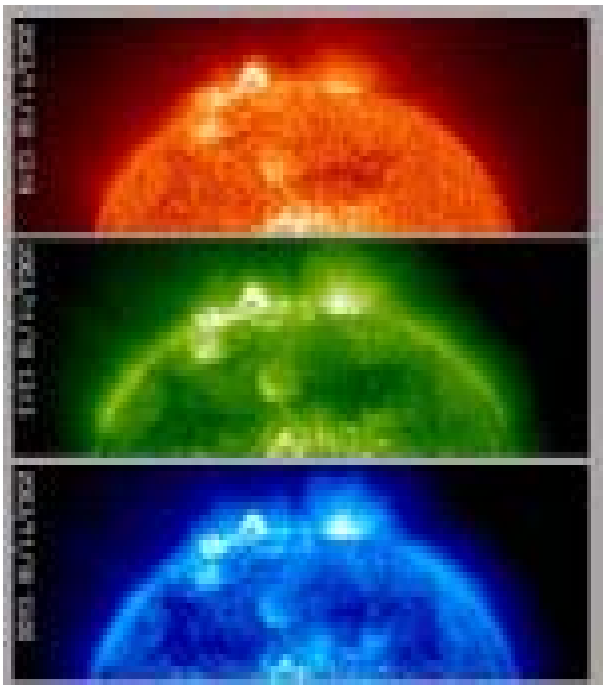

The Aurora seen from space - image courtesy of NASA/ESA

of the electronic and vibrational excitations of NO under auroral conditions. The second set (CSS2) uses the same probabilities for electronic excitation, but the cross sections for ground-state vibrational excitation are based on our recent absolute measurements. The two sets are shown in figure 1 and it is readily apparent that the main difference is the significant level of vibrational excitation in CSS2 at energies below 5 eV. This is due entirely to the enhanced scattering caused by the intermediate NO- resonant state. The peak-like structure in the cross section below 5 eV is due to quasi-vibrational motion of the long-lived negative ions. These large-magnitude, low-energy features were not included in the original CSS1 because, at that stage, the absolute values had not been determined.

Our model calculations were carried out for an IBC II^{+} aurora, at an altitude of 120 km, for infrared emission in the first three fundamental lines of NO. In addition to the electron-driven processes, the chemiluminescent process, and other chemical processes were included. The NO concentration was set at the observed value under IBC II+ conditions of 8.2×10^{8} cm^{-3}. The distribution of electron energies is shown in Figure 2. The results show that when the recently measured vibrational cross sections (CSS2) are employed, the electron-driven processes make a significant contribution, as much as 25%, for each of the three lines, to the overall photon emission rate. This analysis clearly indicates that the origin of the fundamental lines in the infrared spectrum of NO, under auroral conditions, is due to important contributions from *both* chemiluminescent *and* electron - driven phenomena.

Steve Buckman and Milica Jelasavicic in the laboratory

It is intriguing to note the events that lead to the above conclusion. Figures 1 and 2 indicate the strong overlap that occurs between the resonant behaviour in the vibrational excitation cross sections at energies of 0.5-2 eV, and a corresponding 'knee' in the electron energy distribution in the same energy region. It is exactly these electrons that become bound, with high probability, to the NO molecule for a short period of time and then detach themselves with a preference for leaving the molecule in a vibrationally excited state. We note that outside this energy region, and that of a higher-lying resonance at around 15 eV, the vibrational excitation due to direct scattering processes is at least two orders of magnitude smaller. The significant role that electron driven processes play in the IR auroral emissions from NO is thus the result of a serendipitous convergence of molecular structure and the natural distribution of electrons in the upper atmosphere. It demonstrates beautifully how low energy molecular excitation on the angstrom size scale, and the femtosecond time scale, can drive processes occurring across hundreds of kilometres of the upper atmosphere.

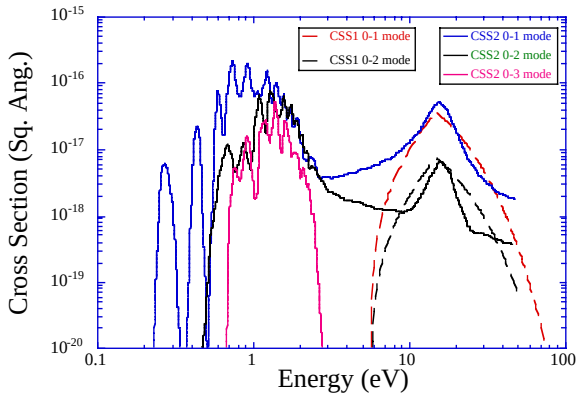

Figure 1. Collision cross section sets used in the present study (CSS2) for the 0-1, 0-2 and 0-3 vibrational modes of NO, compared with those (CSS1) used in the original Auroral model. For clarity, the electronic excitation cross sections, which were common to both sets, are not shown.

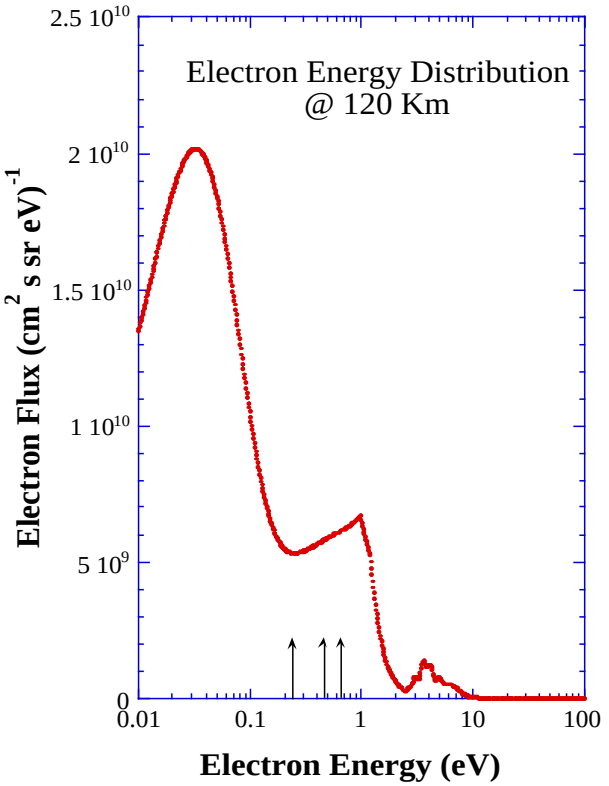

Figure 2. The electron energy distribution function used for the present study. The arrows indicate the threshold energies for the first three vibrational modes of the ground state of NO.

Acknowledgements

This work was a collaborative effort between the Electron Physics Group ANU, and colleagues at Flinders University in Adelaide and the Institute of Physics, Belgrade.